Bioorganic Chemistry 129 (2022) 106127

Contents lists available at ScienceDirect

Bioorganic Chemistry

journal homepage: www.elsevier.com/locate/bioorg

Lactate dehydrogenase A inhibitors with a 2,8-dioxabicyclo[3.3.1]nonane scaffold: A contribution to molecular therapies for primary hyperoxalurias

Alfonso Alejo-Armijo [a], Cristina Cuadrado [a], Joaquin Altarejos [a], Miguel X. Fernandes [b], Eduardo Salido [c,*], Monica Diaz-Gavilan [d], Sofia Salido [a,*]

[a] Departamento de Química Inorgánica y Orgánica, Facultad de Ciencias Experimentales, Universidad de Jaén, Campus de Excelencia Internacional Agroalimentario ceiA3, 23071 Jaén, Spain
[b] Instituto Universitario de Bioorgánica, Universidad de La Laguna, 38206 La Laguna, Spain
[c] Hospital Universitario de Canarias & Center for Rare Diseases (CIBERER), 38320 Tenerife, Spain
[d] Departamento de Química Farmacéutica y Orgánica, Facultad de Farmacia, Universidad de Granada, 18071 Granada, Spain

ARTICLE INFO

Keywords:
Primary hyperoxaluria
Selective lactate dehydrogenase A inhibitors
2,8-Dioxabicyclo[3.3.1]nonane scaffold
Flavylium salts
Hyperoxaluric mouse hepatocytes
Oxalate

ABSTRACT

Human lactate dehydrogenase A (*h*LDHA) is one of the main enzymes involved in the pathway of oxalate synthesis in human liver and seems to contribute to the pathogenesis of disorders with endogenous oxalate overproduction, such as primary hyperoxaluria (PH), a rare life-threatening genetic disease. Recent published results on the knockdown of *LDHA* gene expression as a safe strategy to ameliorate oxalate build-up in PH patients are encouraging for an approach of *h*LDHA inhibition by small molecules as a potential pharmacological treatment. Thus, we now report on the synthesis and *h*LDHA inhibitory activity of a new family of compounds with 2,8-dioxabicyclo[3.3.1]nonane core (**23**–**42**), a series of twenty analogues to A-type proanthocyanidin natural products. Nine of them (**25**–**27**, **29**–**34**) have shown IC_{50} values in the range of 8.7–26.7 μM, based on a UV spectrophotometric assay, where the *h*LDHA inhibition is measured according to the decrease in absorbance of the cofactor β-NADH (340 nm). Compounds **25**, **29**, and **31** were the most active *h*LDHA inhibitors. In addition, the inhibitory activities of those nine compounds against the *h*LDHB isoform were also evaluated, finding that all of them were more selective inhibitors of *h*LDHA versus *h*LDHB. Among them, compounds **32** and **34** showed the highest selectivity. Moreover, the most active *h*LDHA inhibitors (**25**, **29**, **31**) were evaluated for their ability to decrease the oxalate production by hyperoxaluric mouse hepatocytes (PH1, PH2 and PH3) *in vitro*, and the relative oxalate output at 24 h was 16% and 19 % for compounds **25** and **31**, respectively, in *Hoga1*$^{-/-}$ mouse primary hepatocyte cells (a model for PH3). These values improve those of the reference compound used (stiripentol). Compounds **25** and **31** have in common the presence of two hydroxyl groups at rings B and D and an electron-withdrawing group (NO_2 or Br) at ring A, pointing to the structural features to be taken into account in future structural optimization.

1. Introduction

Primary hyperoxaluria (PH) is a rare disease linked to the liver metabolism that results in an overproduction of oxalate anion. The main risk associated with this excess of oxalate is the formation of poorly soluble calcium oxalate (CaOx) crystals and stones in kidneys and urinary tract. The continuous CaOx deposition leads to a remarkable kidney damage and, in most cases, to the consequent end stage renal disease (ESRD). PHs are inherited errors of glyoxylate metabolism and three types of PH (PH1, PH2 and PH3) have been reported. PH1 is the most common and severe form of PH, due to mutations in the *AGXT* gene; PH2 is caused by mutations in the *GRHPR* gene; and PH3 is caused by mutations in the *HOGA1* gene. Loss-of-function mutations in any of these three genes result in a deficit to detoxify glyoxylate, which is then converted into oxalate by hepatic lactate dehydrogenase A (LDHA) [1,2].

Until very recently, the applied treatments were not sufficient to avoid recurring stones or ESRD and, thus, for severe forms of PH, combined liver and kidney transplantation was the only curative treatment [3]. However, current advances in molecular therapy and clinical

* Corresponding authors.
E-mail addresses: esalido@ull.es (E. Salido), ssalido@ujaen.es (S. Salido).

https://doi.org/10.1016/j.bioorg.2022.106127
Received 14 February 2022; Received in revised form 22 May 2022; Accepted 2 September 2022
Available online 8 September 2022

research have led to interesting results for the reduction of the excess systemic oxalate levels in PH. These therapeutic approaches range from targeting molecular defects in the liver to the use of probiotics to enhance oxalate intestinal elimination [4–6]. However, the decreasing of hepatic oxalate synthesis by inhibition of the enzymes involved in the production of oxalate presents a more feasible therapeutic approach. Thus, the inhibition of glycolate oxidase (GO) enzyme [7–9] or hydroxyproline dehydrogenase (HYPDH) enzyme [10,11] are substrate reduction strategies, since both enzymes are involved in the production of glyoxylate. In addition, there is plenty of evidence that supports that the hepatic isozyme lactate dehydrogenase A (LDHA) is the key enzyme responsible for converting glyoxylate to oxalate. Therefore, the inhibition of this enzyme is an attractive strategy in the prevention of oxalate formation for the three types of PH. In fact, two iRNA therapies have been designed to specifically inhibit hepatic expression of *HAO1* gene, which encodes GO enzyme [8], and of *LDHA* gene, which encodes the major isoform of LDH enzyme in the liver (LDHA) [12,13]. As a result, the FDA and EMA agencies approved in November 2020 the first pharmacological treatment for PH1, based on *si*RNA inhibition of GO, for Lumarisan (Alnylam Pharmaceuticals). Thereafter, Nedorisan (Dicerna Pharmaceuticals Inc.), based on *si*RNA inhibition of LDHA, started its phase 3 clinical trial [14]. Results from this ongoing clinical trial using *si*RNA to target liver LDHA expression have not shown significant adverse effects (personal communication, article in preparation) and no safety concerns were raised in the phase I study already published [15].

Once GO and LDHA inhibition with *si*RNA have been clinically validated as a safe therapeutic method for the treatment of PHs [8,13], an alternative or complementary strategy is the inhibition of GO or LDHA by small molecules. These constitute a classical approach and, in contrast to biopharmaceuticals, present the advantage of possible oral administration and, in general, lower production costs. Several patent applications and recent publications have described GO inhibitors (GOi's), most of them sharing the common chemical feature of an aryl carboxylic acid, such as 1,2,3-thiadiazole-4-carboxylic acid [7], 1,2,3-triazole-4-carboxylic acid [16] and more recently salicylic acid derivatives [9] and indazole-3-carboxylic acid [17].

Although LDHA was suggested as a more potent target than GO to reduce urinary oxalate levels [12], to date there are few reports exploring the inhibition of LDHA with small molecules as potential therapeutic agents for PH treatment. Since there are different tetrameric LDH isoforms located in different organs, such as LDHA in skeletal muscle and liver, and LDHB in heart and brain, mainly, a liver organ selective inhibition of *h*LDHA is considered necessary to validate *h*LHDA as a safe therapeutic strategy in PH patients, thus avoiding likely non-desired secondary effects [5].

In a recent study, a patient affected by severe PH1 was treated with a commercial anticonvulsant drug, stiripentol, traded as Diacomit® (Biocodex, France) (Fig. 1), for several weeks showing a decrease of urine oxalate excretion without side effects [18]. However, the effectiveness of this drug seems to depend on the state of the renal function of the patient [19,20]. Forthcoming phase 2 clinical trial (NCT03819647) could yield more information on safety and efficacy of its monotherapy for the treatment of PHs [21].

The hypothesis of double GO/LDHA inhibition leading to more effective and safe drugs has been introduced [5,9,22]. Díaz-Gavilán and col. bet on using the same pharmacophore with a salicylic acid core against both enzymes [22]. Likewise, Lowther and col. have synthesized and evaluated compounds whose structures result from the merger of two scaffolds, one of them is present in a reported GOi and the other one in LDHA inhibitors (LDHAi's) [23].

Given the known role of LDHA in aerobic glycolysis in malignant cells [24], a wide number of LDHAi's have been reported in several review articles [5,25,26] (Fig. 1). Pharmaceutical companies, such as AstraZeneca [27], GlaxoSmithKline [28] and Genentech [29], have developed some of them as potential therapeutics in oncology. However, limitations related to the lack of selectivity or poor pharmacokinetic properties have not led to additional *in vivo* experiments and none of them are currently in clinical trials.

Within the huge structural variability of reported LDHAi's, our attention has been focused on polyphenolic flavone-based inhibitors, such as morin [30], epigallocatechin [31], galloflavin [32] and luteolin-7-*O*-β-D-glucopiranoside [33], which present micromolar IC_{50} values (Fig. 1). These natural products were found to be potential anticancer agents due to their inhibitory activity against *h*LDHA [30–33]. In addition, a LDHA inhibition assay on procyanidin-enriched fractions from *Spatholobus suberectus* extract showed moderate inhibition percentages (55 %) for those fractions predominantly composed of tetrameric to hexameric procyanidins [34].

Procyanidins and other proanthocyanidins are a large group of natural compounds with a 2,8-dioxabicyclo[3.3.1]nonane scaffold, whose biological activities have been evaluated in several occasions [35–40]. However, the ability of compounds with such scaffold to inhibit *h*LDHA has not been studied yet. Thus, according to our knowledge in the synthesis of this kind of compounds [38,39], we report herein the synthesis of a series of 2,8-dioxabicyclo[3.3.1]nonane derivatives, the evaluation of their *h*LDHA and *h*LDHB inhibitory activities, and the *in vitro* assay of a selection of them on hyperoxaluric mouse hepatocytes, in order to find some preliminary structure–activity relationships that help to design more powerful compounds in the future. Regarding the synthetic protocol chosen, most of the reported methods to synthesize these bicyclic compounds use 2-hydroxychalcones as starting materials [41–45], but we have taken advantage of our experience on the

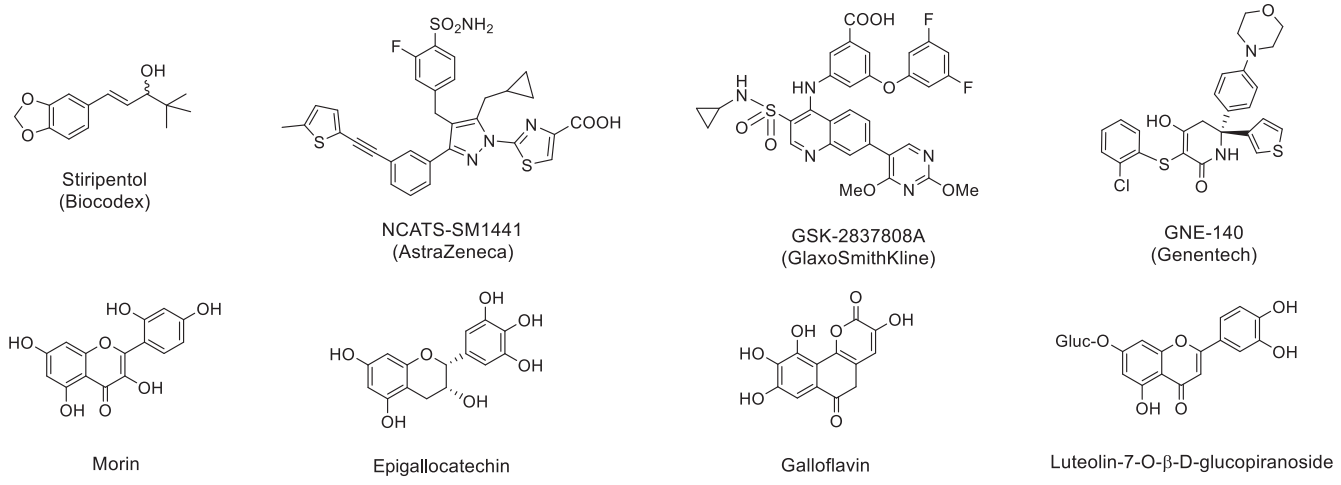

Fig. 1. Structures of some known LDHA inhibitors (LDHAi's).

synthesis of flavylium salts [46] and their use as starting materials [38].

2. Materials and methods

2.1. General experimental methods

All chemicals were purchased and used without further purification, except absolute MeOH and THF, which were prepared and dried, prior to use, according to standard methods [47].

All reactions were carried out under argon atmosphere and at room temperature or in oil baths with electronic temperature control, unless otherwise mentioned. The progress of the reactions was monitored by (a) analytical high-performance liquid chromatography (HPLC) and (b) analytical thin-layer chromatography (TLC) on silica gel 60 F_{254} pre-coated aluminum sheets (0.25 mm, Merck Chemicals, Darmsdadt, Germany) and spots visualized under UV light (254 nm). Purifications of synthesized compounds were performed by semipreparative HPLC or by column chromatography (CC) using Sephadex LH-20 or Silica gel 60 (particle size 0.040–0.063 mm) (Merck Chemicals, Darmsdadt, Germany). Analytical and semipreparative HPLC were conducted on a Waters 600E instrument (Waters Chromatography Division, Milford, MA, USA) equipped with a diode array detector (DAD), scan range: 190–800 nm (Waters CapLC 2996 Photodiode Array Detector, Waters Chromatography Division, Milford, MA, USA), and operating at 30 °C. Analytical HPLC analyses were performed on a C18 reversed-phase Spherisorb ODS-2 column, 250 mm × 3 mm i.d., 5 μm (Waters Chromatography Division, Milford, MA). The best separation was obtained with H_2O:CH_3COOH, 99.8:0.2, v/v (solvent A) and methanol: CH_3COOH, 99.8:0.2, v/v (solvent B) at a flow rate of 0.7 mL/min: linear gradient from 30 % to 100 % B for 25 min; 100 % B for 15 min; and 5 min to return to the initial conditions. The total run time excluding equilibration was 45 min. Purity of the compounds was assessed by analytical HPLC at 280 nm on the C18 reversed-phase described above (data are included in the Supplementary Material section).

Semipreparative HPLC separations were performed on a C18 reversed-phase Spherisorb ODS-2 column, 250 mm × 10 mm i.d., 5 μm (Waters Chromatography Division, Milford, MA) at a flow rate of 5 mL/min.

Infrared (IR) spectra were recorded on a Bruker Tensor 27 Fourier transform infrared (FTIR) spectrometer (Bruker Optik GmbH, Ettlingen, Germany) using an Attenuated Total Reflectance (ATR) accessory, and only characteristic absorptions (ν, cm^{-1}) are reported. ^1H NMR and ^{13}C NMR spectra were recorded on a Bruker Avance 400 spectrometer (Bruker Daltonik GmbH, Bremen, Germany) operating at 400 and 100 MHz for ^1H and ^{13}C, respectively. Deuterated methanol (CD_3OD) was used to prepare solutions of purified compounds for NMR. For flavylium salts a drop of DCl was added to ensure acid conditions. The chemical shifts (in ppm) were referenced to solvent peaks as internal reference. The coupling constants (J) are quoted in hertz (Hz). The following abbreviations are used: *d*, doublet; *t*, triplet; *m*, multiplet; *br s*, broad singlet; *br d*, broad doublet; *dd*, doublet of doublets; *ddd*, doublet of doublet of doublets; *td*, triplet of doublets; *dq*, doublet of quartets. The complete assignment of ^1H and ^{13}C signals was performed by analysis of the correlated homonuclear (COSY) and heteronuclear (HMBC, HSQC) 2D NMR spectra. High-resolution mass spectra (HRMS) were recorded on an Agilent 6520B Quadrupole time-of-flight (QTOF) mass spectrometer (Agilent Technologies, Santa Clara, CA, USA) with an electrospray ionization (ESI) interface operating in positive or negative mode.

2.2. General method A for the synthesis of flavylium salts (**10**–**19**)

A mixture of the salicylic aldehyde derivative (2 mmol), the acetophenone or propiophenone derivative (2 mmol), 98 % H_2SO_4 (0.6 mL; 10.8 mmol) and HOAc (2.6 mL) was stirred overnight at room temperature according to procedures previously used by us [38,39,46]. Then, Et_2O (30 mL) was added and a reddish solid precipitated. The solid was filtered off and carefully washed with Et_2O and dried. The flavylium salts **10** (0.605 g, 90 % yield), **11** (0.506 g, 79 % yield), **12** (0.586 g, 77 % yield), **13** (0.555 g, 76 % yield) and **14** (0.672 g, 85 % yield) were described previously with similar yields and their structures confirmed by comparison of their spectral data with those reported in the literature: **10** [48], **11** [49], **12** [39], **13** [50], and **14** [38].

2.2.1. 3-Methyl-4′-hydroxy-6-nitroflavylium hydrogen sulfate (**15**)

Method A was followed by using 2-hydroxy-6-nitrobenzaldehyde (**2**) (0.334 g, 2 mmol) and 4′-hydroxypropiophenone (**9**) (0.300 g, 2 mmol). Pure compound **15** was obtained as a red–orange solid (0.690 g, 91 % yield). Melting point: 260 °C (decomposes); ^1H NMR (400 MHz, DCl/CD_3OD, pD ≈ 1.0) δ 8.11–8.00 (*m*, 2H, H-4, H-7), 7.33–7.20 (*m*, 2H, H-2′, H-6′), 6.98 (*d*, J = 8.4, 1H, H-8), 6.79–6.74 (*m*, 2H, H-3′, H-5′), 6.73 (*br s*, 1H, H-5), 1.66 (*d*, J = 1.3, 3H, CH_3); ^{13}C NMR (100 MHz, DCl/CD_3OD, pD ≈ 1.0) δ 159.3 (C-2, C-4′), 159.1 (C-9), 143.4 (C-6), 134.9 (C-3), 133.4 (C-10), 128.9 (C-2′, C-6′), 125.8 (C-7), 123.9 (C-5), 123.1 (C-4), 116.8 (C-8), 116.1 (C-3′, C-5′), 106.8 (C-1′), 19.1 (CH_3); FT-IR (ATR) ν_{max}: 3069, 1589, 1535, 1489, 1408, 1308, 1277, 1165, 1119, 1055, 943, 862, 824, 750, 706, 681 cm^{-1}; HRMS (ESI-TOF) m/z $[M]^+$ Calcd. for $C_{16}H_{12}NO_4$ 282.0766, found 282.0762.

2.2.2. 3′,4′-Dihydroxy-6-chloroflavylium hydrogen sulfate (**16**)

Method A was followed by using 2-hydroxy-5-chlorobenzaldehyde (**3**) (0.313 g, 2 mmol) and 3′,4′-dihydroxyacetophenone (**6**) (0.304 g, 2 mmol). Pure compound **16** was obtained as a red-brownish solid (0.608 g, 79 % yield). Melting point: 245 °C (decomposes); ^1H NMR (400 MHz, DCl/CD_3OD, pD ≈ 1.0) δ 9.09 (*d*, J = 9.3, 1H, H-4), 8.63 (*d*, J = 9.3, 1H, H-3), 8.28 (*d*, J = 2.5, 1H, H-5), 8.26 (*d*, J = 9.1, 1H, H-8), 8.21 (*dd*, J = 8.8, 2.4, 1H, H-6′), 8.13 (*dd*, J = 9.1, 2.5, 1H, H-7), 7.98 (*d*, J = 2.4, 1H, H-2′), 7.13 (*d*, J = 8.8, 1H, H-5′); ^{13}C NMR (100 MHz, DCl/CD_3OD, pD ≈ 1.0) δ 176.0 (C-2), 160.3 (C-4′), 154.9 (C-9), 152.8 (C-4), 148.7 (C-3′), 138.7 (C-7), 135.8 (C-6), 130.0 (C-5), 129.8 (C-6′), 125.6 (C-10), 121.9 (C-8), 121.3 (C-1′), 119.6 (C-3), 118.7 (C-5′), 117.3 (C-2′); FT-IR (ATR) ν_{max} 3373, 3088, 1630, 1593, 1543, 1504, 1448, 1339, 1313, 1145, 1119, 1032, 908, 885, 817, 796, 784 cm^{-1}; HRMS (ESI-TOF) m/z $[M]^+$ Calcd. for $C_{15}H_{10}ClO_3$ 273.0318, found 273.014.

2.2.3. 4′-Hydroxy-6-chloroflavylium hydrogen sulfate (**17**)

Method A was followed by using 2-hydroxy-5-chlorobenzaldehyde (**3**) (0.313 g, 2 mmol) and 4′-hydroxyacetophenone (**7**) (0.272 g, 2 mmol). Pure compound **17** was obtained as a red–orange solid (0.447 g, 63 % yield). Melting point: 235 °C (decomposes); ^1H NMR (400 MHz, DCl/CD_3OD, pD ≈ 1.0) δ 9.19 (*d*, J = 9.3 Hz, 1H, H-4), 8.71 (*d*, J = 9.3 Hz, 1H, H-3), 8.67–8.57 (*m*, 2H, H-2′, H-6′), 8.40–8.26 (*m*, 2H, H-5, H-8), 8.16 (*dd*, J = 9.1 Hz, J = 2.4 Hz, 1H, H-7), 7.19 (*m*, 2H, H-3′, H-5′); ^{13}C NMR (100 MHz, DCl/CD_3OD, pD ≈ 1.0) δ 177.0 (C-2), 170.7 (C-4′), 155.2 (C-9), 153.8 (C-4), 139.1 (C-7), 136.6 (C-2′, C-6′), 136.1 (C-6), 130.3 (C-5), 125.8 (C-10), 122.1 (C-8), 121.0 (C-1′), 119.6 (C-3), 119.5 (C-3′, C-5′); FT-IR (ATR) ν_{max}: 3153, 3089, 1610, 1581, 1539, 1500, 1450, 1375, 1331, 1311, 1269, 1176, 1157, 1137, 1126, 1116, 1049, 941, 856, 810, 688 cm^{-1}; HRMS (ESI-TOF) m/z $[M]^+$ Calcd. for $C_{15}H_{10}ClO_2$ 257.0369, found 257.0366.

2.2.4. 3′,4′-Dihydroxy-6-bromoflavylium hydrogen sulfate(**18**)

Method A was followed by using 2-hydroxy-5-bromobenzaldehyde (**4**) (0.402 g, 2 mmol) and 3′,4′-dihydroxyacetophenone (**6**) (0.304 g, 2 mmol). Pure compound **18** was obtained as a red-brownish solid (0.744 g, 90 % yield). Melting point: 272 °C (decomposes); ^1H NMR (400 MHz, DCl/CD_3OD, pD ≈ 1.0) δ 9.08 (*d*, J = 9.3,1H, H-4), 8.64 (*d*, J = 9.3, 1H, H-3), 8.45 (*d*, J = 2.3, 1H, H-5), 8.27–8.19 (*m*, 3H, H-7, H-8, H-6′), 8.00 (*d*, J = 2.3, 1H, H-2′), 7.15 (*d*, J = 8.7, 1H, H-5′); ^{13}C NMR (100 MHz, DCl/CD_3OD, pD ≈ 1.0) δ 175.6 (C-2), 160.3(C-4′), 155.3 (C-9), 152.5(C-4), 148.8 (C-3′), 141.4 (C-7), 133.3 (C-5), 123.5 (C-6), 129.9 (C-6′), 126.0 (C-10), 121.9 (C-8), 121.3 (C-1′), 119.6 (C-3), 118.7 (C-5′),

117.3 (C-2′); FT-IR (ATR) ν_{max}: 3153, 3089, 1610, 1581, 1539, 1500, 1450, 1331, 1311, 1269, 1176, 1157, 1137, 1126, 1116, 1049, 941, 856, 810, 688 cm^{-1}; HRMS (ESI-TOF) *m/z* $[M]^+$ Calcd. for $C_{15}H_{10}BrO_3$ 316.9813, found 316.9809.

2.2.5. 4′-Hydroxy-6-bromoflavylium hydrogen sulfate (19)

Method A was followed by using 2-hydroxy-6-bromobenzaldehyde (**4**) (0.402 g, 2 mmol) and 4′-hydroxyacetophenone (**7**) (0.272 g, 2 mmol). Pure compound **19** was obtained as a red–orange solid (0.545 g, 68 % yield). Melting point: 235 °C (decomposes); ^{1}H NMR (400 MHz, DCl/CD_3OD, pD ≈ 1.0) *δ* 9.18 (*d*, *J* = 9.2, 1H, H-4), 8.68 (*d*, *J* = 9.2, 1H), 8.64–8.55 (*m*, 2H, H-2′, H-6′), 8.48 (*d*, *J* = 2.2, 1H, H-5), 8.28 (*dd*, *J* = 9.0, 2.2, 1H, H-7), 8.23 (*d*, *J* = 9.0, 1H, H-8), 7.21 (*d*, *J* = 8.9, 2H, H-3′, H-5′); ^{13}C NMR (100 MHz, DCl/CD_3OD, pD ≈ 1.0) *δ* 175.4 (C-2), 170.3 (C-4′), 155.4 (C-9), 153.8 (C-4), 142.1 (C-7), 136.8 (C-2′, C-6′), 133.6 (C-5), 126.1 (C-10), 124.8 (C-6), 122.3 (C-8), 121.1 (C-1′), 119.6 (C-3, C-3′, C-5′); FT-IR (ATR) ν_{max}: 3153, 3089, 1610, 1581, 1539, 1500, 1450, 1375, 1331, 1311, 1269, 1176, 1157, 1137, 1126, 1116, 1049, 941, 856, 810, 688 cm^{-1}; HRMS (ESI-TOF) *m/z* $[M]^+$ Calcd. for $C_{15}H_{10}BrO_2$ 300.9864, found 300.9859.

2.3. Method B for the synthesis of 3′,4′-dihydroxy-6-carboxyflavylium chloride (20)

A mixture of 2-hydroxy-5-carboxybenzaldehyde (**5**) (0.332 g, 2 mmol) and 3′,4′-dihydroxyacetophenone (**6**) (0.304 g, 2 mmol) in absolute EtOH (40 mL) was saturated with dry HCl (g) for 1 h. The reaction mixture was stirred overnight following a similar method to that described by Kraus *et al* [51]. Then, the solvent was removed, Et_2O (30 mL) was added and a solid precipitated. The solid was filtered off and carefully washed with Et_2O and dried. Pure compound **20** was obtained as a brownish solid (0.449 g, 96 % yield). Melting point: 235 °C (decomposes); ^{1}H NMR (400 MHz, DCl/CD_3OD, pD ≈ 1.0) *δ* 9.17 (*d*, *J* = 8.5, 1H, H-4), 8.79 (*d*, *J* = 1.2, 1H, H-5), 8.64 (*br d*, *J* = 8.5, 2H, H-3, H-7), 8.31 (*d*, *J* = 8.5, 1H, H-8), 8.25 (*br d*, *J* = 8.7, 1H, H-6′), 8.02 (*br s*, 1H, H-2′), 7.15 (*d*, *J* = 8.7, 1H, H-5′); This compound is not soluble and stable enough to record a ^{13}C NMR spectrum; FT-IR (ATR) ν_{max}: 3500, 1712, 1596, 1552, 1506, 1458, 1033 cm^{-1}; HRMS (ESI-TOF) *m/z* $[M]^+$ Calcd. for $C_{16}H_{11}O_5$ 283.0606, found 283.0602.

2.4. General method C for the synthesis of 2,8-dioxabicyclo[3.3.1]nonanes (23–42)

A mixture of flavylium salt (**10**–**20**) (0.5 mmol) and phloroglucinol (**21**) or resorcinol (**22**) (0.5 mmol) in absolute MeOH (8 mL) (or absolute THF for compounds **34** and **42**) was stirred overnight at 50 °C following a similar method to that described by Kraus *et al.* [54] and used previously by us [38,39]. Then, the solvent was removed and the crude purified by semipreparative HPLC or by CC using Sephadex LH-20 or Silica gel 60. The dioxabicyclic derivatives **23** (0.069 g, 34 % yield from the starting aldehyde **1**), **25** (0.170 g, 64 % from **2**) and **27** (0.170 g, 63 % from **2**) were described previously with similar yields and their structures confirmed by comparison of their spectral data with those reported in the literature: **23** [54], **25** [54] and **27** [38]. Analytical HPLC (*λ* = 280 nm): compound **23** (purity: 98 %; t_R = 15.9 min); compound **25** (purity: 97 %; t_R = 21.2 min); compound **27** (purity: 94 %; t_R = 17.9 min).

2.4.1. 2-(4′-Hydroxyphenyl)chromane-(4 → 4,2 → O-5)-phloroglucinol (24)

Method C was followed by using the flavylium salt **11** (0.140 g) and phloroglucinol (**21**, 0.063 g, 0.5 mmol). Then, the solvent was removed and the crude purified by semipreparative HPLC. Purification eluting with MeOH-H_2O (50:50) yielded pure analogue **24** as a white amorphous solid (0.032 g, 22 % from **1**). Melting point: 155 °C (decomposes); ^{1}H NMR (400 MHz, CD_3OD) *δ* 7.49 (*m*, 2H, H-2′(B), H-6′(B)), 7.38 (*dd*, *J* = 7.5, 1.7, 1H, H-5(A)), 7.07 (*ddd*, *J* = 8.0, 7.5, 1.7, 1H, H-7(A)), 6.89 (*dd*, *J* = 8.0, 1.1, 1H, H-8(A)), 6.82 (*m*, 3H, H-6(A), H-3′(B), H-5′(B)), 5.93 (*m*, 2H, H-2″(D), H-6″(D)), 4.35 (*t*, *J* = 3.1, 1H, H-4(C)), 2.20 (*d*, *J* = 3.1, 2H, H-3(C));^{13}C NMR (100 MHz, CD_3OD) *δ* 159.1 (C-4′(B)), 158.3* (C-1″(D)), 156.4* (C-5″(D)), 154.9* (C-3″(D)), 153.9 (C-9(A)), 134.8 (C-1′(B)), 129.5 (C-10(A)),129.1 (C-5(A)), 128.6 (C-7(A)),128.4 (C-2′(B), C-6′(B)), 122.2 (C-6(A)), 117.1 (C-8(A)), 116.1 (C-3′(B), C-5′(B)), 107.6 (C-4″(D)), 100.3 (C-2(C)), 97.1$^{\#}$ (C-2″(D)), 96.0$^{\#}$ (C-6″(D)), 35.1 (C-3(C)), 28.4 (C-4(C)) ($^{*,\#}$these signals could be interchanged); FT-IR (ATR) v_{max}: 3300, 2960, 2931, 1606, 1514, 1475, 1437, 1336, 1300, 1230, 1171, 1117, 1062, 1009, 885, 811, 783 cm^{-1}; HRMS (ESI-TOF) *m/z* $[M-H]^-$ Calcd. for $C_{21}H_{16}O_5$ 348.0998, found 348.1002. Analytical HPLC (*λ* = 280 nm): purity: 93 %; t_R = 18.1 min.

2.4.2. 2-(4′-Hydroxyphenyl)-6-nitrochromane-(4 → 4,2 → O-5)-phloroglucinol (26)

Method C was followed by using the flavylium salt **13** (0.195 g) and phloroglucinol (**21**, 0.063 g, 0.5 mmol). Then, the solvent was removed and the crude purified by silica gel CC. Purification eluting with DCM-EtOH (97:3) yielded pure analogue **26** as a white amorphous solid (0.088 g, 45 % from **2**). Melting point: 170 °C (decomposes); ^{1}H NMR (400 MHz, CD_3OD) *δ* 8.29 (*d*, *J* = 2.8, 1H, H-5(A)), 7.99 (*dd*, *J* = 9.1, 2.8, 1H, H-7(A)), 7.50 (*d*, *J* = 8.9, 2H, H-2′(B), H-6′(B)), 7.02 (*d*, *J* = 9.1, 1H, H-8(A)), 6.84 (*d*, *J* = 8.9, 2H, H-3′(B), H-5′(B)), 5.96(*br s*, 2H, H-2″(D), H-6″(D)), 4.47 (*t*, *J* = 3.0, 1H, H-4(C)), 2.30 (*m*, 2H, H-3(C)); ^{13}C NMR (100 MHz, CD_3OD) *δ* 159.6 (C-9(A)), 159.3 (C-4′(B)), 158.7 (C-3″(D)), 156.4 (C-1″(D)), 154.1 (C-5″(D)), 142.8 (C-6(A)), 133.4 (C-1′(B)), 130.4 (C-10(A)), 128.2 (C-2′(B), C-6′(B)), 124.6 (C-5(A), C-7(A)), 117.7 (C-8(A)), 116.1 (C-3′(B), C-5′(B)), 106.0 (C-4″(D)), 101.2 (C-2(C)), 97.24* (C-2″(D)), 96.0* (C-6″(D)), 33.9 (C-3(C)), 28.2 (C-4(C)) (*these signals could be interchanged); FT-IR (ATR) v_{max}: 3300, 2945, 2912, 1602, 1508, 1475, 1330, 1242, 1170, 1124, 1085, 1064, 1006, 970, 889, 817, 746 cm^{-1}; HRMS (ESI-TOF) *m/z* $[M-H]^-$ Calcd. for $C_{21}H_{14}NO_7$ 392.0776, found 392.0780. Analytical HPLC (*λ* = 280 nm): purity: 98 %; t_R = 19.4 min.

2.4.3. 2-(4′-Hydroxyphenyl)-3-methyl-6-nitrochromane-(4 → 4,2 → O-5)-phloroglucinol (28)

Method C was followed by using the flavylium salt **15** (0.200 g) and phloroglucinol (**21**, 0.063 g, 0.5 mmol). Then, the solvent was removed and the crude purified by silica gel CC. Purification eluting with DCM-EtOH (97:3) yielded pure analogue **28** as a white amorphous solid (0.102 g, 50 % from **2**). Melting point: 280 °C (decomposes); ^{1}H NMR (400 MHz, CD_3OD) *δ* 8.27 (*d*, *J* = 2.7, 1H, H-5(A)), 7.98 (*dd*, *J* = 8.9, 2.7, 1H, H-7(A)), 7.45 (*d*, *J* = 8.9, 2H, H-2′(B), H-6′(B)), 6.96 (*d*, *J* = 8.9, 1H, H-8(A)), 6.85 (*d*, *J* = 8.9, 2H, H-3′(B), H-5′(B)), 6.02* (*d*, *J* = 2.3, 1H, H-6″(D)), 5.99* (*d*, *J* = 2.3, 1H, H-2″(D)), 4.23 (*d*, *J* = 2.3, 1H, H-4(C)), 2.42 (*dq*, *J* = 6.4, 2.3, 1H, H-3(C)), 0.77 (*d*, *J* = 6.4, 2H, CH_3); ^{13}C NMR (100 MHz, CD_3OD) *δ* 159.6 (C-9(A)), 159.1 (C-3″(D)), 158.6 (C-4′(B)), 157.1 (C-1″(D)), 153.1 (C-5″(D)), 142.5 (C-6(A)), 131.9 (C-10(A)), 131.7 (C-1′(B)), 128.7 (C-2′(B), C-6′(B)), 124.4 (C-7(A)), 124.0 (C-5(A)), 117.2 (C-8(A)), 115.8 (C-3′(B), C-5′(B)), 104.0 (C-2(C)), 103.1 (C-4″(D)), 97.5 (C-2″(D)), 95.6 (C-6″(D)), 35.5 (C-3(C)), 34.3 (C-4(C)), 13.8 (CH_3) (*these signals could be interchanged); FT-IR (ATR) v_{max}: 3396, 3168, 1608, 1502, 1477, 1330, 1247, 1209, 1168, 1132, 1083, 1051, 1002, 916, 821, 748, 692 cm^{-1}; HRMS (ESI-TOF) *m/z* $[M-H]^-$ Calcd. for $C_{22}H_{16}NO_7$ 406.0932, found 406.0933. Analytical HPLC (*λ* = 280 nm): purity: 98 %; t_R = 19.8 min.

2.4.4. 2-(3′,4′-Dihydroxyphenyl)-6-chlorochromane-(4 → 4,2 → O-5)-phloroglucinol (29)

Method C was followed by using the flavylium salt **16** (0.185 g, 0.5 mmol) and phloroglucinol (**21**, 0.063 g, 0.5 mmol). Then, the solvent was removed and the crude purified by silica gel CC. Purification eluting with DCM-EtOH (97:3) yielded pure analogue **29** as a colorless foam (0.084 g, 43 % from **3**). ^{1}H NMR (400 MHz, CD_3OD) *δ* 7.34 (*d*, *J* = 2.7,

1H, H-5(A)), 7.10 (*d*, *J* = 2.3, 1H, H-2′(B)), 7.03 (*dd*, *J* = 8.7, 2.7, 1H, H-7(A)), 6.98 (*dd*, *J* = 8.3, 2.3, 1H, H-6′(B)), 6.86 (*d*, *J* = 8.7, 1H, H-8(A)), 6.80 (*d*, *J* = 8.3, 1H, H-5′(B)), 5.95* (*d*, *J* = 2.1, 1H, H-6″(D)), 5.94* (*d*, *J* = 2.1, 1H, H-2″(D)), 4.32 (*t*, *J* = 3.1, 1H, H-4(C)), 2.21[#] (*dd*, *J* = 13.4, 3.1, 1H, H-3b (C)), 2.18[#] (*dd*, *J* = 13.4, 3.1, 1H, H-3a (C)); ^{13}C NMR (100 MHz, CD_3OD) δ 158.6[‡] (C-1″(D)), 156.4[‡] (C-5″(D)), 154.7 (C-3″(D)), 152.8 (C-9(A)), 147.1 (C-4′(B)), 146.3 (C-3′(B)), 135.0 (C-1′(B)), 131.4 (C-10 (A)), 128.6 (C-5 (A)), 128.3 (C-7(A)), 126.7 (C-6(A)), 118.6 (C-8(A), C-6′(B)), 116.2 (C-5′(B)), 114.5 (C-2′ (B)), 106.8 (C-4″(D)), 100.4 (C-2(C)), 97.2 (C-6″(D)), 96.1 (C-2″(D)), 34.7 (C-3(C)), 28.4 (C-4 (C)) (*,#,‡ these signals could be interchanged); FT-IR (ATR) v_{max}: 3549, 3474, 3414, 2925, 2856, 1636, 1617, 1520, 1480, 1338, 1301, 1234, 1119, 1058, 817, 619 cm^{-1}; HRMS (ESI-TOF) *m/z* $[M-H]^-$ Calcd. for $C_{21}H_{15}ClO_6$ 397.0484, found 397.0487. Analytical HPLC (λ = 280 nm): purity: 99 %; t_R = 18.8 min.

2.4.5. 2-(4′-Hydroxyphenyl)-6-chlorochromane-(4 → 4,2 → O-5)-phloroglucinol (30)

Method C was followed by using the flavylium salt **17** (0.171 g) and phloroglucinol (**21**, 0.063 g, 0.5 mmol). Then, the solvent was removed and the crude purified by semipreparative HPLC. Purification eluting with MeOH-H_2O (60:40) yielded pure analogue **30** as a colorless foam (0.077 g, 42 % from **3**). ^{1}H NMR (400 MHz, CD_3OD) δ 7.52–7.43 (*m*, 2H, H-2′(B), H-6′(B)), 7.35 (*d*, *J* = 2.6, 1H, H-5(A)), 7.04 (*dd*, *J* = 8.6, 2.6, 1H, H-7(A)), 6.87 (*d*, *J* = 8.6, 1H, H-8(A)), 6.85–6.78 (*m*, 2H, H-3′(B), H-5′(B)), 5.95* (*d*, *J* = 2.2, 1H, H-2″(D)), 5.93* (*d*, *J* = 2.2, 1H, H-6″(D)), 4.33 (*t*, *J* = 3.1, 1H, H-4(C)), 2.21 (*dd*, *J* = 13.4, 3.1, 2H, H-3(C)); ^{13}C NMR (100 MHz, CD_3OD) δ 159.3 (C-4′(B)), 158.7[#] (C-1″(D)), 156.5[#] (C-5″(D)), 154.8[#] (C-3″(D)), 152.8 (C-9(A)), 134.4 (C-1′(B)), 131.4 (C-10 (A)), 128.6 (C-5 (A)), 128.3 (C-7(A), C-2′(B), C-6′(B)), 126.8 (C-6(A)), 118.7 (C-8(A)), 116.2 (C-3′(B), C-5′(B)), 106.8 (C-4″(D)), 100.5 (C-2 (C)), 97.2 (C-6″(D)), 96.1 (C-2″(D)), 34.6 (C-3(C)), 28.4 (C-4(C)) (*, #these signals could be interchanged); FT-IR (ATR) v_{max}: 3300, 2960, 2931, 1606, 1514, 1475, 1437, 1336, 1300, 1230, 1171, 1117, 1062, 1009, 885, 811, 783 cm^{-1}; HRMS (ESI-TOF) *m/z* $[M-H]^-$ Calcd. for $C_{21}H_{15}ClO_5$ 382.0608, found 382.0609. Analytical HPLC (λ = 280 nm): purity: 96 %; t_R = 20.7 min.

2.4.6. 2-(3′,4′-Dihydroxyphenyl)-6-bromochromane-(4 → 4,2 → O-5)-phloroglucinol (31)

Method C was followed by using the flavylium salt **18** (0.208 g, 0.5 mmol) and phloroglucinol (**21**, 0.063 g, 0.5 mmol). Then, the solvent was removed and the crude purified by semipreparative HPLC. Purification eluting with MeOH-H_2O (60:40) yielded pure analogue **31** as a brown syrup (0.096 g, 41 % from **4**). ^{1}H NMR (400 MHz, CD_3OD) δ 7.48 (*d*, *J* = 2.5, 1H, H-5(A)), 7.17 (*dd*, *J* = 8.7, 2.5, 1H, H-7(A)), 7.11 (*d*, *J* = 2.1, 1H, H-2′(B)), 6.98 (*dd*, *J* = 8.3, 2.1, 1H, H-6′(B)), 6.82 (*d*, *J* = 8.7, 1H, H-8(A)),6.80 (*d*, *J* = 8.3, 1H, H-5′(B)), 5.95* (*d*, *J* = 2.3, 1H, H-6″(D)), 5.94* (*d*, *J* = 2.3, 1H, H-2″(D)), 4.31 (*t*, *J* = 3.0, 1H, H-4(C)), 2.21[#] (*dd*, *J* = 13.4, 3.0, 1H, H-3β (C)), 2.17[#] (*dd*, *J* = 13.4, 3.0, 1H, H-3α (C)). ^{13}C NMR (100 MHz, CD_3OD) δ 158.6 (C-1″(D)), 156.4 (C-5″(D)), 154.7 (C-3″(D)), 153.3 (C-9(A)), 147.1 (C-4′(B)), 146.3 (C-3′(B)), 135.0 (C-1′(B)), 131.9 (C-10 (A)), 131.5 (C-5 (A)), 131.3 (C-7(A)), 119.1 (C-8 (A)), 118.6 (C-6′(B)), 116.2 (C-5′(B)), 114.5 (C-2′ (B)), 114.0 (C-6(A)), 106.8 (C-4″(D)), 100.4 (C-2(C)), 97.2 (C-6″(D)), 96.1 (C-2″(D)), 34.7 (C-3(C)), 28.4 (C-4(C)). (*,#these signals could be interchanged); FT-IR (ATR) v_{max}: 3300, 1606, 1514, 1475, 1436, 1336, 1299, 1230, 1116, 1062, 1008, 885, 811 cm^{-1}; HRMS (ESI-TOF) *m/z* $[M-H]^-$ Calcd. for $C_{21}H_{15}BrO_6$ 440.9979, found 440.9980. Analytical HPLC (λ = 280 nm): purity: 99 %; t_R = 19.3 min.

2.4.7. 2-(4′-Hydroxyphenyl)-6-bromochromane-(4 → 4,2 → O-5)-phloroglucinol (32)

Method C was followed by using the flavylium salt **19** (0.191 g) and phloroglucinol (**21**, 0.063 mg, 0.5 mmol). Then, the solvent was removed and the crude purified by semipreparative HPLC. Purification eluting with MeOH-H_2O (60:40) yielded pure analogue **32** as a white foam (0.100 g, 49 % from **4**). ^{1}H NMR (400 MHz, CD_3OD) δ 7.67–7.32 (*m*, 3H, H-5(A), H-2′(B), H-6′(B)), 7.14 (*dd*, *J* = 8.7, 2.5, 1H, H-7(A)), 6.92–6.65 (*m*, 3H, H-8(A), H-3′(B), H-5′(B)), 5.92* (*d*, *J* = 2.3, 1H, H-6″(D)), 5.91* (*d*, *J* = 2.3, 1H, H-2″(D)), 4.29 (*t*, *J* = 3.1, 1H, H-4(C)), 2.17 (*dd*, *J* = 13.4, 3.1, 2H, H-3(C)); ^{13}C NMR (100 MHz, CD_3OD) δ 159.2 (C-4′(B)), 158.6[#] (C-1″(D)), 156.4[#] (C-5″(D)), 154.7[#] (C-3″(D)), 153.3 (C-9 (A)), 134.4 (C-1′(B)), 131.9 (C-10 (A)), 131.5 (C-5 (A)), 131.3 (C-7(A)), 128.4 (C-2′(B), C-6′(B)), 119.1 (C-8(A)), 116.1 (C-3′(B), C-5′(B)), 114.0 (C-6(A)), 106.8 (C-4″(D)), 100.5 (C-2(C)), 97.2 (C-6″(D)), 96.1 (C-2″ (D)), 34.6 (C-3(C)), 28.3 (C-4(C)) (*,#these signals could be interchanged); FT-IR (ATR) v_{max}: 3300, 2960, 2931, 1606, 1514, 1475, 1437, 1336, 1300, 1230, 1171, 1117, 1062, 1009, 885, 811, 783 cm^{-1}; HRMS (ESI-TOF) *m/z* $[M-H]^-$ Calcd. for $C_{21}H_{15}BrO_5$ 426.0103, found 426.0104. Analytical HPLC (λ = 280 nm): purity: 96 %; t_R = 21.1 min.

2.4.8. 2-(3′,4′-Dihydroxyphenyl)-6-carboxymethylchromane-(4 → 4,2 → O-5)-phloroglucinol (33) and 2-(3′,4′-dihydroxyphenyl)-6-carboxychromane-(4 → 4, 2 → O-5)-phloroglucinol (34)

Method C was followed by using the flavylium salt **20** (0.300 g, 0.94 mmol) and phloroglucinol (**21**, 0.200 g, 1.58 mmol). Then, the solvent was removed and the crude purified by silica gel CC. Purification eluting with DCM-MeOH (97:3) yielded pure analogue **33** as white foam (0.241 g, 58 % from **5**) and **34** as a brownish syrup (0.036 mg, 9 % from **5**). When THF was used as solvent instead of MeOH, the pure analogue **34** was formed as the only product (0.204 g, 51 % from **5**).Compound **33**: ^{1}H NMR (400 MHz, CD_3OD) δ 8.11 (*d*, *J* = 2.2, 1H, H-5(A)), 7.79 (*dd*, *J* = 8.5, 2.2, 1H, H-7(A)), 7.15 (*d*, *J* = 2.2, 1H, H-2′(B)), 7.03 (*dd*, *J* = 8.3, 2.2, 1H, H-6′(B)), 6.98 (*d*, *J* = 8.5, 1H, H-8(A)), 6.84 (*d*, *J* = 8.3, 1H, H-5′(B)), 5.97 (*br s*, 2H, H-2″(D), H-6″(D)), 4.44 (*t*, *J* = 3.1, 1H, H-4(C)), 3.22 (*s*, 3H, $COO\underline{CH_3}$), 2.32–2.22 (*m*, 2H, H-3(C)). ^{13}C NMR (100 MHz, CD_3OD) δ 168.6 ($\underline{COO}CH_3$), 158.3* (C-1″D), 158.2 (C-9(A)), 156.3* (C-5″(D)), 154.3 (C-3″(D)), 146.9 (C-4′(B)), 146.1 (C-3′(B)), 134.9 (C-1′(B)), 130.7 (C-5(A)), 130.3 (C-7(A)), 129.6 (C-10 (A)), 123.8 (C-6(A)), 118.3 (C-6′(B)), 117.1 (C-8(A)), 116.0 (C-5′(B)), 114.2 (C-2′(B)), 106.6 (C-4″(D)), 100.5 (C-2(C)), 97.0[#] (C-6″(D)), 95.8[#](C-2″(D)), 52.4 ($COO\underline{CH_3}$), 34.5 (C-3(C)), 28.1 (C-4(C)).(*,#these signals could be interchanged); FT-IR (ATR) v_{max}: 3295, 2923, 2850, 1687, 1608, 1515, 1438, 1274, 1195, 1170, 1114, 1064, 1010, 899, 819, 767, 719 cm^{-1}; HRMS (ESI-TOF) *m/z* $[M-H]^-$ Calcd. for $C_{23}H_{18}O_8$ 421.0929, found 421.0934. Analytical HPLC (λ = 280 nm): purity: 95 %; t_R = 25.1 min. Compound **34**: ^{1}H NMR (400 MHz, CD_3OD) δ 8.10 (*d*, *J* = 2.1, 1H, H-5 (A)), 7.78 (*dd*, *J* = 8.5, 2.1, 1H, H-7(A)), 7.12 (*d*, *J* = 2.2, 1H, H-2′(B)), 7.00 (*dd*, *J* = 8.3, 2.2, 1H, H-6′(B)), 6.96 (*d*,*J* = 8.5,1H, H-8(A)), 6.81 (*d*, *J* = 8.3, 1H, H-5′(B)), 5.95 (*br s*, 1H, H-2″(D)), 5.95 (*br s*, 1H, H-6″(D)), 4.42 (*t*, *J* = 2.9, 1H, H-4(C)), 2.27 (*dd*, *J* = 13.3, 2.9, 1H, H-3β (C)), 2.23 (*dd*, *J* = 13.3, 2.9, 1H, H-3α(C)). ^{13}C NMR (100 MHz, CD_3OD) δ 170.2 (COOH), 158.6* (C-1″(D)), 158.3 (C-9(A)), 156.5* (C-5″(D)), 154.5 (C-3″(D)), 147.1 (C-4′(B)), 146.3 (C-3′(B)), 134.9 (C-1′(B)), 131.3 (C-5 (A)), 130.8 (C-7(A)), 129.7 (C-10 (A)), 124.6 (C-6(A)), 118.6 (C-6′(B)),117.2 (C-8(A)), 116.2 (C-5′(B)), 114.5 (C-2′ (B)), 106.9 (C-4″(D)), 100.8 (C-2 (C)), 97.3[#] (C-6″(D)), 96.0[#] (C-2″(D)), 34.8 (C-3(C)), 28.4 (C-4(C)) (*, #these signals could be interchanged); FT-IR (ATR) v_{max}: 3309, 1685, 1608, 1515, 1438, 1184, 1109, 1066 cm^{-1}; HRMS (ESI-TOF) *m/z* $[M-H]^-$ Calcd. for $C_{22}H_{16}O_8$ 407.0772, found 407.0774. Analytical HPLC (λ = 280 nm): purity: 99 %; t_R = 13.9 min.

2.4.9. 2-(3′,4′-Dihydroxyphenyl)-6-nitrochromane-(4 → 4,2 → O-3)-resorcinol (35)

Method C was followed by using the flavylium salt **12** (0.191 g) and resorcinol (**22**, 0.059 g, 0.5 mmol). Then, the solvent was removed and the crude purified by silica gel CC. Purification eluting with DCM-EtOH (97:3) yielded pure analogue **35** as a white amorphous solid (0.098 g, 50 % from **2**). Melting point: 145 °C (decomposes); ^{1}H NMR (400 MHz, CD_3OD) δ 8.22 (*d*, *J* = 2.7, 1H, H-5(A)), 8.00 (*dd*, *J* = 9.0, 2.7, 1H, H-7 (A)), 7.15 (*d*, *J* = 9.1, 1H, H-5″(D)), 7.13 (*d*, *J* = 2.3, 1H, H-2′(B)), 7.03

(*d*, $J = 9.0$, 1H, H-8(A)), 7.00 (*dd*, $J = 8.3$, 2.3, 1H, H-6′(B)), 6.82 (*d*, $J = 8.3$, 1H, H-5′(B)), 6.40 (*m*, 2H, H-2″(D), H-6″(D)), 4.17 (*t*, $J = 3.1$, 1H, H-4(C)), 2.35 (*dd*, $J = 13.4$, 3.1, 2H, H-3(C)); ^{13}C NMR (100 MHz, CD_3OD) δ 159.2 (C-1″(D)), 159.1 (C-9(A)), 153.3 (C-3″(D)), 147.2 (C-4′(B)), 146.2 (C-3′(B)), 143.2 (C-6(A)), 133.8 (C-1′(B)), 130.3 (C-10(A)), 129.4 (C-5″(D)), 128.1 (C-8(A)), 124.9 (C-7(A)), 124.3 (C-5(A)), 118.4 (C-6′(B)), 118.2 (C-4″(D)), 116.1 (C-5′(B)), 114.3 (C-2′(B)), 110.7* (C-6″(D)), 104.4* (C-2″(D)), 100.9 (C-2(C)), 34.4 (C-4(C)), 34.2 (C-3(C)) (*these signals could be interchanged); FT-IR (ATR) v_{max}: 3296, 2912, 1595, 1477, 1433, 1330, 1292, 1249, 1147, 1107, 1083, 1016, 966, 810, 784, 771, 746, 688 cm^{-1}; HRMS (ESI-TOF) *m/z* $[M-H]^-$ Calcd. for $C_{21}H_{14}NO_7$ 392.0776, found 392.0777. Analytical HPLC ($\lambda = 280$ nm): purity: 94 %; $t_R = 17.8$ min.

2.4.10. 2-(4′-Hydroxyphenyl)-6-nitrochromane-(4 → 4,2 → O-3)-resorcinol (36)

Method C was followed by using the flavylium salt **13** (0.195 g) and resorcinol (**22**, 0.059 g, 0.5 mmol). Then, the solvent was removed and the crude purified by crystallization in a mixture of Et_2O:hexane yielding pure analogue **36** as a white amorphous solid (0.121 g, 64 % from **2**). Melting point: 85 °C (decomposes); ^{1}H NMR (400 MHz, CD_3OD) δ 8.21 (*d*, $J = 2.7$, 1H, H-5(A)), 7.97 (*dd*, $J = 8.9$, 2.7, 1H, H-7(A)), 7.50 (*d*, $J = 8.9$, 2H, H-2′(B), H-6′(B)), 7.13 (*d*, $J = 9.1$, 1H, H-5″(D)), 7.01 (*d*, $J = 8.9$, 1H, H-8(A)), 6.84 (*d*, $J = 8.9$, 2H, H-3′(B), H-5′(B)), 6.41(*br s*,1H, H-2″(D)), 6.40 (*dd* overlapped, $J = 9.1$, 2.5, 1H, H-6″(D)), 4.14 (*t*, $J = 3.1$, 1H, H-4(C)), 2.33 (*dd*, $J = 13.4$, 3.1, 2H, H-3(C)); ^{13}C NMR (100 MHz, CD_3OD) δ 159.3* (C-9(A)), 159.1* (C-4′(B)), 159.0 (C-1″(D)), 153.6 (C-3″(D)), 143.1 (C-6(A)), 133.1 (C-1′(B)), 130.2 (C-10(A)), 129.4 (C-5″(D)), 128.2 (C-2′(B), C-6′(B)), 124.9 (C-7(A)), 124.2 (C-5(A)), 118.1 (C-8(A), C-4″(D)), 116.1 (C-3′(B), C-5′(B)), 110.7 (C-6″(D)), 104.4 (C-2″(D)), 101.0 (C-2(C)), 34.4 (C-4(C)), 34.0 (C-3(C)) (*these signals could be interchanged); FT-IR (ATR) v_{max}: 3317, 2916, 2842, 1585, 1502, 1477, 1330, 1247, 1147, 1107, 1083, 102, 999, 958, 887, 823, 746, 688, 638 cm^{-1}; HRMS (ESI-TOF) *m/z* $[M-H]^-$ Calcd. for $C_{21}H_{14}NO_6$ 376.0827, found 376.0827. Analytical HPLC ($\lambda = 280$ nm): purity: 95 %; $t_R = 19.7$ min.

2.4.11. 2-(3′,4′-Dihydroxyphenyl)-3-methyl-6-nitrochromane-(4 → 4,2 → O-3)-resorcinol (37)

Method C was followed by using the flavylium salt **14** (0.200 g) and resorcinol (**22**, 0.059 g, 0.5 mmol). Then, the solvent was removed and the crude purified by silica gel CC. Purification eluting with DCM-EtOH (97:3) yielded pure analogue **37** as a white amorphous solid (0.122 g, 60 % from **2**). Melting point: 182 °C (decomposes); ^{1}H NMR (400 MHz, CD_3OD) δ 8.22 (*d*, $J = 2.7$, 1H, H-5(A)), 8.01 (*dd*, $J = 9.0$, 2.7, 1H, H-7(A)), 7.15 (*d*, $J = 8.1$, 1H, H-5″(D)), 7.08 (*d*, $J = 2.3$, 1H, H-2′(B)), 6.97 (*m*, 2H, H-8(A), H-6′(B)), 6.84 (*d*, $J = 8.3$, 1H, H-5′(B)), 6.46 (*d*, $J = 2.3$, 1H, H-2″(D)), 6.44 (*dd*, $J = 8.1$, 2.3, 1H, H-6″(D)), 3.95 (*d*, $J = 2.5$, 1H, H-4(C)), 2.45 (*dd*, $J = 13.4$, 2.5, 2H, H-3(C)), 0.78 (*d*, $J = 6.8$, 3H, CH_3); ^{13}C NMR (100 MHz, CD_3OD) δ 159.2 (C-9(A)), 158.9 (C-1″(D)), 152.6 (C-3″(D)), 147.0 (C-4′(B)), 146.0 (C-3′(B)), 142.8 (C-6(A)), 132.0 (C-1′(B), C-10(A)), 130.5 (C-5″(D)), 124.8 (C-7(A)), 123.6 (C-5(A)), 119.0 (C-6′(B)), 117.5 (C-8(A)), 115.8 (C-5′(B)), 115.3 (C-4″(D)), 114.7 (C-2′(B)), 111.0 (C-6″(D)), 104.0 (C-2″(D)), 103.8 (C-2(C)), 40.5 (C-4(C)), 35.6 (C-3(C)), 13.8 (CH_3); FT-IR (ATR) v_{max}: 3346, 2960, 2910, 1591, 1502, 1477, 1434, 1330, 1247, 1143, 1101, 1008, 974, 916, 889, 823, 779, 744, 688 cm^{-1}; HRMS (ESI-TOF) *m/z* $[M-H]^-$ Calcd. for $C_{22}H_{16}NO_7$ 406.0932, found 406.0937. Analytical HPLC ($\lambda = 280$ nm): purity: 94 %; $t_R = 18.3$ min.

2.4.12. 2-(4′-Hydroxyphenyl)-3-methyl-6-nitrochromane-(4 → 4,2 → O-3)-resorcinol (38)

Method C was followed by using the flavylium salt **15** (0.200 g) and resorcinol (**22**, 0.059 g, 0.5 mmol) Then, the solvent was removed and the crude purified by silica gel CC. Purification eluting with DCM-MeOH (98:2) yielded pure analogue **38** as a white amorphous solid (0.131 g, 64 % from **2**). Melting point: 250 °C (decomposes); ^{1}H NMR (400 MHz, CD_3OD) δ 8.28 (*d*, $J = 2.8$, 1H, H-5(A)), 8.06 (*dd*, $J = 9.0$, 2.8, 1H, H-7(A)), 7.53–7.49 (*m*, 2H, H-2′(B)), 7.20 (*d*, $J = 8.2$, 1H, H-5″(D)), 7.03 (*d*, $J = 9.0$, 1H, H-8(A)), 6.92–6.87 (*m*, 2H, H-3″(D)), 6.51 (*d*, $J = 2.4$, 1H, H-2″(D)), 6.48 (*dd*, $J = 8.2$, 2.4, 1H, H-6″(D)), 4.03 (*d*, $J = 2.5$, 1H, H-4(C)), 2.54 (qd, $J = 6.9$, 2.5, 1H, H-3(C)), 0.82 (*d*, $J = 6.9$, 3H, CH_3). ^{13}C NMR (100 MHz, CD_3OD) δ 159.5 (C-4′(B), C-9(A)), 159.3 (C-1″(D)), 152.9 (C-3″(D)), 143.2 (C-6(A)), 132.3 (C-10(A)), 131.7 (C-1′(B)), 130.9 (C-5″(D)), 129.0 (C-2′(B)), 125.1 (C-7(A)), 123.9 (C-5(A)), 117.9 (C-8(A)), 116.1 (C-3′(B)), 115.6 (C-4″(D)), 111.4 (C-6″(D)), 104.4 (C-2″(D)), 104.2 (C-2(C)), 40.8 (C-4(C)), 35.9 (C-3(C)), 14.09 (CH_3); FT-IR (ATR) v_{max}: 3396, 3170; 2916, 2842, 1585, 1502, 1477, 1330, 1247, 1147, 1107, 1083, 102, 999, 958, 887, 823, 746, 688, 638 cm^{-1}; HRMS (ESI-TOF) *m/z* $[M-H]^-$ Calcd. for $C_{22}H_{16}NO_6$ 390.0983, found 390.0982. Analytical HPLC ($\lambda = 280$ nm): purity: 98 %; $t_R = 20.2$ min.

2.4.13. 2-(3′,4′-Dihydroxyphenyl)-6-chlorochromane-(4 → 4,2 → O-3)-resorcinol (39)

Method C was followed by using the flavylium salt **16** (0.185 g) and resorcinol (**22**, 0.055 g, 0.5 mmol). Then, the solvent was removed and the crude purified by semipreparative HPLC. Purification eluting with MeOH-H_2O (60:40) yielded pure analogue **39** as a brown syrup (0.065 g, 36 % from **3**). ^{1}H NMR (400 MHz, CD_3OD) δ 7.27 (*d*, $J = 2.5$, 1H, H-5(A)), 7.11 (*d*, $J = 2.1$, 1H, H-2′(B)), 7.09–7.04 (*m*, 2H, H-7(A), H-5″(D)), 6.99 (*dd*, $J = 8.3$, 2.1, 1H, H-6′(B)), 6.87 (*d*, $J = 8.7$,1H, H-8(A)), 6.81 (*d*, $J = 8.3$, 1H, H-5′(B)), 6.38–6.36 (*m*, 2H, H-2″(D), H-5″(D)), 3.99 (*t*, $J = 3.0$,1H, H-4(C)), 2.28* (*dd*, $J = 13.5$, 3.0, 1H, H-3b (C)), 2.25* (*dd*, $J = 13.5$, 3.0, 1H, H-3a (C)); ^{13}C NMR (100 MHz, CD_3OD) δ 158.9 (C-1″(D)), 154.2 (C-3″(D)), 152.4 (C-9(A)), 147.1 (C-4′(B)), 146.3 (C-3′(B)), 134.8 (C-1′(B)), 131.1 (C-10 (A)), 129.3 (C-5″(D)), 128.2 (C-5 (A)), 128.8 (C-7(A)), 127.1 (C-6(A)), 119.0 (C-8(A)), 118.8 (C-6′(B)), 116.2 (C-5′(B)), 114.5 (C-2′ (B)), 114.1 (C-4″(D)), 110.4 (C-6″(D)), 104.4 (C-2″(D)), 100.4 (C-2(C)), 34.8 (C-3(C), C-4(C)) (*these signals could be interchanged); FT-IR (ATR) v_{max}: 3319, 1606, 1508, 1479, 1334, 1249, 1126, 1085, 1008, 813 cm^{-1}; HRMS (ESI-TOF) *m/z* $[M-H]^-$ Calcd. for $C_{21}H_{15}ClO_5$ 381.0535, found 381.0538. Analytical HPLC ($\lambda = 280$ nm): purity: 98 %; $t_R = 20.6$ min.

2.4.14. 2-(3′,4′-Dihydroxyphenyl)-6-bromochromane-(4 → 4,2 → O-3)-resorcinol (40)

Method C was followed by using the flavylium salt **18** (0.208 g) and resorcinol (**22**, 0.055 g, 0.5 mmol). Then, the solvent was removed and the crude purified by semipreparative HPL. Purification eluting with MeOH-H_2O (60:40) yielded pure analogue **40** as a brown reddish syrup (0.054 g, 35 % from **4**). ^{1}H NMR (400 MHz, CD_3OD) δ 7.40 (*d*, $J = 2.5$, 1H, H-5(A)), 7.18 (*dd*, $J = 8.7$, 2.5, 1H, H-7(A)), 7.11 (*d*, $J = 2.1$, 1H, H-2′(B)), 7.07 (*d*, $J = 8.9$, 1H, H-5″(D)), 6.98 (*dd*, $J = 8.3$, 2.1, 1H, H-6′(B)), 6.82 (*d*, $J = 8.7$, 1H, H-8(A)), 6.80 (*d*, $J = 8.3$, 1H, H-5′(B)), 6.38–6.36 (*m*, 2H, H-2″(D), H-6″(D)), 3.99–3.97 (*m*, 1H, H-4(C)), 2.27* (*dd*, $J = 13.7$, 2.9, 1H, H-3b (C)), 2.23* (*dd*, $J = 13.7$, 2.9, 1H, H-3a (C)); ^{13}C NMR (100 MHz, CD_3OD) δ 158.9 (C-1″(D)), 154.2 (C-3″(D)), 152.9 (C-9(A)), 147.1 (C-4′(B)), 146.3 (C-3′(B)), 134.7 (C-1′(B)), 131.7 (C-10 (A)), 131.8 (C-7(A)), 131.1 (C-5 (A)), 129.4 (C-5″(D)), 119.5 (C-8(A)), 119.0 (C-4″(D)), 118.6 (C-6′(B)), 116.2 (C-5′(B)), 114.5 (C-2′ (B)), 114.3 (C-6(A)), 100.3 (C-2(C)), 110.4 (C-6″(D)), 104.4 (C-2″(D)), 34.8 (C-3(C)), 34.7 (C-4(C)) (*these signals could be interchanged); FT-IR (ATR) v_{max}: 3300, 1606, 1514, 1475, 1116, 1062, 1008, 811 cm^{-1}; HRMS (ESI-TOF) *m/z* $[M-H]^-$ Calcd. for $C_{21}H_{15}BrO_5$ 425.003, found 425.0031. Analytical HPLC ($\lambda = 280$ nm): purity: 96 %; $t_R = 25.8$ min.

2.4.15. 2-(3′,4′-Dihydroxyphenyl)-6-carboxymethylchromane-(4 → 4,2 → O-3)-resorcinol (41) and 2-(3′,4′-dihydroxyphenyl)-6-carboxychromane-(4 → 4,2 → O-3)-resorcinol (42)

Method C was followed by using the flavylium salt **20** (0.290 g) and resorcinol (**22**, 0.090 g, 0.82 mmol). Then, the solvent was removed and the crude purified by silica gel CC. Purification eluting with DCM-MeOH

(97:3) yielded pure analogue **41** as white foam (0.169 g, 44 % from **5**) and **42** as a brownish syrup (0.026 g, 7 % from **5**). When THF was used as solvent instead of MeOH, the pure analogue **42** was formed as the sole product (0.087 g, 30 % from **5**). Compound **41**: ^{1}H NMR (400 MHz, CD_3OD) δ 7.98 (*d*, $J = 2.1$, 1H, H-5(A)), 7.80 (*dd*, $J = 8.5$, 2.1, 1H, H-7 (A)), 7.15 (*d*, J = 2.3, 1H, H-2′(B)), 7.13 (*d*, J = 7.9, 1H, H-5″(D)), 7.03 (*dd*, J = 8.3, 2.3, 1H, H-6′(B)), 7.00 (*d*, $J = 8.5$, 1H, H-8(A)), 6.85 (*d*, $J = 8.3$, 1H, H-5′(B)), 6.43–6.38 (m, 2H, H-2″(D), H-6″(D)), 4.12 (*t*, $J = 2.9$, 1H, H-4(C)), 3.88 (*s*, 3H, COO$\underline{CH_3}$), 2.38–2.30 (*m*, 2H, H-3(C)); ^{13}C NMR (100 MHz, CD_3OD) δ 168.4 ($\underline{COO}$Me), 158.7 (C-1″(D)), 157.7 (C-9(A)), 153.7 (C-3″(D)), 147.0 (C-4′(B)), 146.1 (C-3′(B)), 134.2 (C-1′ (B)), 130.6 (C-7(A)), 130.2 (C-5 (A)), 129.4 (C-10 (A)), 129.1 (C-5″(D)), 124.2 (C-6(A)), 118.9 (C-4″(D)), 118.3 (C-6′(B)), 117.4 (C-8(A)), 116.0 (C-5′(B)), 114.2 (C-2′ (B)), 110.2 (C-6″(D)), 104.2 (C-2″(D)), 100.5 (C-2 (C)), 52.4 ($\underline{COO}$Me), 34.6 (C-3(C)), 30.7 (C-4(C)). FT-IR (ATR) ν_{max}: 3319, 2974, 1681, 1606, 1504, 1436, 1284, 1259, 1236, 1195, 1153, 1147, 1107, 1018, 968, 896, 840, 769 cm^{-1}; HRMS (ESI-TOF) *m/z* [M−H]$^-$ Calcd. for $C_{23}H_{18}O_7$ 405.0980, found 405.0981. Analytical HPLC ($\lambda = 280$ nm): purity: 99 %; $t_R = 28.7$ min. Compound **42**: ^{1}H NMR (400 MHz, CD_3OD) δ 7.97 (*d*, $J = 2.1$, 1H, H-5(A)), 7.80 (*dd*, $J = 8.5$, 2.1, 1H, H-7(A)), 7.13–7.11 (*m,* 2H, H-2′(B), H-5″(D)), 7.01 (*dd*, $J = 8.3$, 2.2,1H, H-6′(B)), 6.98 (*d*, $J = 8.5$, 1H, H-8(A)), 6.82 (*d*, $J = 8.3$,1H, H-5′ (B)), 6.40–6.37 (*m,* 2H, H-2″(D), H-6″(D)), 4.11 (*t*, $J = 2.9$, 1H, H-4(C)), 2.35* (*dd*, $J = 14.0$, 2.9, 1H, H-3b (C)), 2.31* (*dd*, $J = 14.0$, 2.9, 1H, H-3a (C)); ^{13}C NMR (100 MHz, CD_3OD) δ 170.0 (COOH), 158.9 (C-1″(D)), 157.9 (C-9(A)), 154.0 (C-3″(D)), 147.2 (C-4′(B)), 146.4 (C-3′(B)), 134.6 (C-1′(B)), 131.2 (C-7(A)), 130.7 (C-5 (A)), 129.5 (C-10 (A)), 129.4 (C-5″ (D)), 125.1 (C-6(A)), 119.2 (C-4″(D)), 118.6 (C-6′(B)), 117.6 (C-8(A)), 116.3 (C-5′(B)), 114.5 (C-2′ (B)), 110.5 (C-6″(D)), 104.5 (C-2″(D)), 100.7 (C-2(C)), 35.0 (C-3(C)), 34.9 (C-4(C)) (*these signals could be interchanged); FT-IR (ATR) ν_{max}: 3300, 1684, 1610, 1506, 1440, 1153, 1107, 1020, 970 cm^{-1}; HRMS (ESI-TOF) *m/z* [M−H]$^-$ Calcd. for $C_{22}H_{16}O_7$ 391.0823, found 391.0828. Analytical HPLC ($\lambda = 280$ nm): purity: 93 %; $t_R = 15.9$ min.

2.5. Human lactate dehydrogenase A enzymatic activity assay

Enzymatic activity of *h*LDHA was determined with recombinant human LDHA (95 %, specific activity > 300 units/mg and concentration of 0.5 mg/mL, Abcam, Cambridge, United Kingdom) in the presence of sodium pyruvate (96 %, Merck) as substrate and β-NADH (≥97 %, Merck) as cofactor in 100 mM potassium phosphate buffer, pH 7.4. The enzymatic assay was performed on 96-well microplates and the decrease in the β-NADH absorbance (340 nm) was measured in a *Synergy HT* Multi-Detector Microplate Reader (BioTeK Instrument, Inc.) for 10 min at 28 °C. The activity was determined using the method employed by Li *et al.* [34] and modified as described here: in each well, the final volume was set to 200 μL and the final concentrations were 100 mM potassium phosphate buffer, 0.041 units/mL LDHA, 155 μM β-NADH, 1 mM pyruvate (saturated conditions), and DMSO solutions (1 %, v/v) of pure compounds at concentrations in the range of 0.09–200 μM. The reaction was initiated by the addition of pyruvate and a suitable linear timeframe was selected to calculate the slope of each concentration. Controls for the establishment of the 0 % and 100 % enzymatic activity were introduced in the assay and the compound 3-[[3[(*cyclopropylamino*)*sulfonyl*]-7-(2,4-dimethoxy-5-pyrimidinyl)-4-quinolinyl]amino]-5-(3,5-difluorophenoxy)benzoic acid (GSK 2,837,808 A, Tocris, Minneapolis, USA) was used as a positive control at 1 μM in well [28]. All measurements were made in triplicate and data were expressed as the mean ± SD and plotted in GraphPad Prism version 5.00 for Windows (GraphPad Software, La Jolla, California, USA). Nonlinear regression analysis was used for dose response curve, fitting of logarithm of inhibitor concentration *vs* normalized enzymatic activity, to calculate IC_{50} values (separate graphs, used to calculate IC_{50} values for each compound, have been included in the Supplementary Material section).

2.6. Human lactate dehydrogenase B enzymatic activity assay

Enzymatic activity of *h*LDHB was determined with recombinant human LDHB (95 %, specific activity > 300 units/mg and concentration of 1.0 mg/mL, Abcam, Cambridge, United Kingdom) following the same protocol described in subsection 2.5.

2.7. Lipophilicity and cell membrane permeability

Calculated log P (ClogP) has been estimated using the MOE computational tool [52].

2.8. Mouse hepatocytes isolation and culture

Hepatocytes were isolated *in situ* by collagenase perfusion method from male C57BL/6 *Agxt1*$^{-/-}$ *Grhpr*$^{-/-}$ and *Hoga1*$^{-/-}$ mouse livers [53]. A total of 2.5×10^6 cells/well were cultured in six-well plates with Williams E medium (Thermo Fisher, Whaltham, USA) supplemented with 5 % fetal bovine serum (Thermo Fisher), 2 mM L-glutamine, 100 U/mL penicillin, 100 μg/mL streptomycin, 2.2 mUI/mL insulin, 2.5 μg/mL amphotericin B and 0.3 μg/mL hydrocortisone. After 24 h, medium was changed to serum-free Williams E medium. High levels of metabolic substrates (5 mM glycolate, 10 mM glycolate and 10 mM hydroxyproline) were used in these short-term cultures to enhance production of oxalate in *Agxt1*$^{-/-}$, *Grhpr*$^{-/-}$ and *Hoga1*$^{-/-}$ primary hepatocyte cultures, respectively [7]. Under these conditions, oxalate accumulates in the media of hyperoxaluric hepatocytes in a time-dependent manner. Culture media was collected at 24 and 48 h after addition of inhibitors to measure the amount of oxalate excreted by the *Agxt1*$^{-/-}$, *Grhpr*$^{-/-}$ or *Hoga1*$^{-/-}$ hepatocytes.

2.9. Cell viability and cytotoxicity

96-Well plates were seeded with 1.0×10^4 cells/well and treated with the same concentrations of compounds as in 6-well plates. At each time point, 20 μL of Cell Titer 96® Aqueous One Solution Reagent (Promega, Madison, WI, USA) was added to the medium, incubated 2 h at 37 °C, 5 % CO_2, and absorbance measured at 490 nm. Relative cellular viability at a concentration of 10 μM for each inhibitor was calculated from the concentration of colored MTS formazan (3-(4,5-dimethylthiazol-2-yl)-5-(3-carboxymethoxyphenyl)-2-(4-sulfophenyl)–2H-tetrazolium) found in wells treated with the inhibitor by comparison with the concentration of formazan found in wells without added inhibitor (negative controls). Each relative cellular viability value for every inhibitor was calculated as an average of three replicates. Values showed a cell death below 3 % at 24 h and 48 h [7].

2.10. Oxalate determination

Oxalate excreted to the medium was measured with an oxalate oxidase assay kit (Greiner Diagnostic GmbH, Bahlingen, Germany), following manufacturer's instructions. The method involves oxidation of oxalate (1 equiv) by oxalate oxidase with formation of H_2O_2 (1 equiv) and subsequent utilization of the generated H_2O_2 for the formation of a dye (absorbance at 590 nm) in a HRP (horseradish peroxidase) catalyzed reaction with the substrates 3-methyl-2-benzothiazolinone hydrazone (MBTH) and 3-(dimethylamino)benzoic acid (DMAB). For oxalate quantification, a standard curve was constructed using aqueous dilutions of oxalate containing 0, 0.025, 0.05, 0.1, 0.2 and 0.25 nmol/μL ($R^2 = 0.9978$). For the standard curve, absorbance was measured at 590 nm following the same protocol described above [9].

Relative oxalate for each inhibitor at the concentration of 10 μM was calculated from the concentration of extracellular oxalate found in wells treated with the inhibitor, as a percentage of the extracellular oxalate found in wells without added inhibitor (negative controls). Each relative oxalate value for every inhibitor was calculated as an average of three replicates.

3. Results and discussion

3.1. Chemical synthesis

According to our experience in the synthesis of flavylium salts [46] and the influence of the electronic features of flavylium salts on their reactivity with nucleophiles to yield bicyclic adducts [38], we have selected for this work several electron-withdrawing groups at A-ring, such as NO_2, halogens, COOH, and COOMe. Thus, the two-step synthetic method followed to obtain 2,8-dioxabicyclo[3.3.1]nonane derivatives (**23**–**42**) is based on the addition of a commercial oxygenated aromatic nucleophile, phloroglucinol (**21**) or resorcinol (**22**), to flavylium salts (**10**–**20**), electrophilic compounds previously synthesized (Scheme 1).

The synthesis of those flavylium (1-benzopyrylium) salts was performed by aldol condensation in acid media between salicylic aldehyde (**1**) and derivatives (**2**–**5**) and acetophenone or propiophenone derivatives (**6**–**9**) according to procedures previously used by us [38,41,46]. Most of the flavylium salts (**10**–**19**) were obtained with moderate to high yield (63–91 %) using CH_3CO_2H/conc. H_2SO_4 4:1 (v/v) as acid media (Method A, entries 1–10 in Table 1). However, salt **20** could not be prepared in proper yield under these conditions, and a second method using ethanol saturated with gaseous hydrogen chloride had to be followed to get a high yield of **20** (96 %, Method B, entry 11 in Table 1). The substitution pattern of rings A, B, and C in the flavylium salts was designed taking into account two key structural features: (1) hydroxyl groups are present in all polyphenolic scaffold-based LDHAi's [25], (2) electron-withdrawing groups at A-ring provide adequate electronic densities in the aromatic system in order to achieve the second step of the synthesis of dioxabicyclo derivatives [38]. Thus, flavylium salts with NO_2, Cl, Br, COOH groups at the A-ring and one OH group or a catechol moiety at the B-ring have been synthesized (**12**–**20**) in addition to flavylium salts with non-substituted A-rings (**10**, **11**).

The addition of phloroglucinol (**21**) or resorcinol (**22**) to flavylium salts (**10**–**20**) was performed following a similar procedure to that described in the literature [54] and previously used by us [38,41]. Thus, the corresponding flavylium salts were mixed with one equivalent of phloroglucinol or resorcinol, and the reaction was carried out in absolute methanol or tetrahydrofuran at 50 °C (Method C, entries 12–31 in Table 1, the yields were calculated from starting aldehydes). The highest yields obtained in these reactions (45–64 %) corresponded to 2,8-dioxabicyclo[3.3.1]nonane derivatives with a NO_2 group at A-ring (**25**–**28** and **35**–**38**). Other derivatives (**29**–**34** and **39**–**42**) with electron-withdrawing groups at A-ring (Cl, Br, COOH or COOMe) were obtained with moderate yield (30–58 %), and other derivatives, like **23** and **24**, with no substituents at A-ring, were obtained with lower yields (34 % and 22 %, respectively). The use of methanol as solvent in the reaction between flavylium salt **20** and phloroglucinol (**21**) or resorcinol (**22**) promoted, after the formation of 2,8-dioxabicyclo[3.3.1]nonane derivatives, the esterification reaction between the carboxylic group and methanol, catalyzed by traces of acid from the flavylium salts. In this reaction conditions, the corresponding methyl ester derivatives **33** and **41** were the main reaction products (58 % and 44 % yield, respectively; entries 22 and 30 in Table 1) and carboxylic derivatives **34** and **42** were obtained with low yields (9 % and 7 %, respectively). However, it was possible to obtain **34** and **42** with moderate yields (51 % and 30 %, respectively, entries 23 and 31 in Table 1) following the same procedure, but changing methanol by tetrahydrofuran. The largest nucleophilic character of phloroglucinol (**21**) versus resorcinol (**22**) was

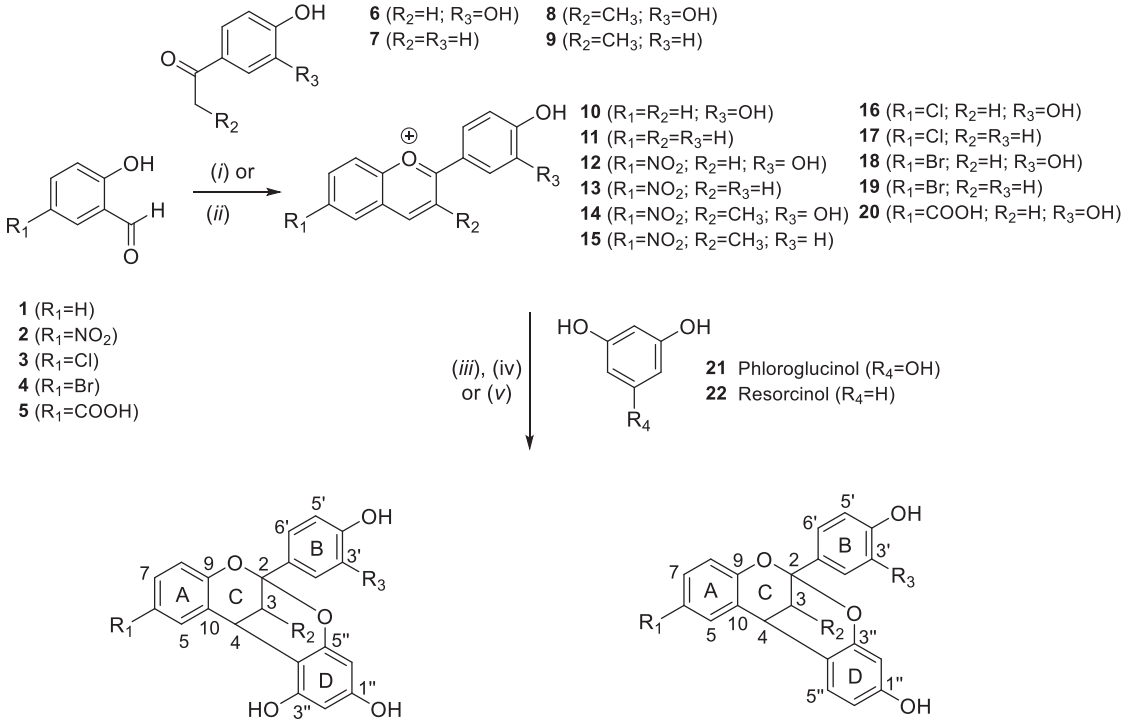

Scheme 1. Synthesis of flavylium salts (**10**–**20**) and 2,8-dioxabicyclo[3.3.1]nonane derivatives (**23**–**42**). Reagents and conditions: (*i*) H_2SO_4, HOAc; (*ii*) EtOH, HCl (g); (*iii*) MeOH, 50 °C, 24 h; (*iv*) MW, MeOH, 80 °C, 20 min; (*v*) MW, MeOH/aq buffer (pH 5.8), 100 °C.

Table 1
Reaction yields in the synthesis of flavylium salts **10**–**20** and dioxabicycles **23**–**42**.

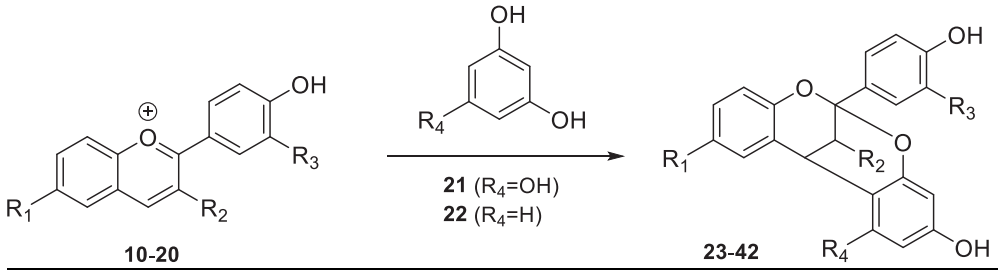

entry	compound	R_1	R_2	R_3	R_4	synthetic method	yield (%) [a]
1	**10**	H	H	OH	–	A	90
2	**11**	H	H	H	–	A	79
3	**12**	NO_2	H	OH	–	A	77
4	**13**	NO_2	H	H	–	A	76
5	**14**	NO_2	CH_3	OH	–	A	85
6	**15**	NO_2	CH_3	H	–	A	91
7	**16**	Cl	H	OH	–	A	79
8	**17**	Cl	H	H	–	A	63
9	**18**	Br	H	OH	–	A	90
10	**19**	Br	H	H	–	A	68
11	**20**	COOH	H	OH	–	B	96
12	**23**	H	H	OH	OH	C	34
13	**24**	H	H	H	OH	C	22
14	**25**	NO_2	H	OH	OH	C	64
15	**26**	NO_2	H	H	OH	C	45
16	**27**	NO_2	CH_3	OH	OH	C	63
17	**28**	NO_2	CH_3	H	OH	C	50
18	**29**	Cl	H	OH	OH	C	43
19	**30**	Cl	H	H	OH	C	42
20	**31**	Br	H	OH	OH	C	41
21	**32**	Br	H	H	OH	C	49
22	**33**	COOMe	H	OH	OH	C	58
23	**34**	COOH	H	OH	OH	C	(9) 51 [b]
24	**35**	NO_2	H	OH	H	C	50
25	**36**	NO_2	H	H	H	C	64
26	**37**	NO_2	CH_3	OH	H	C	60
27	**38**	NO_2	CH_3	H	H	C	64
28	**39**	Cl	H	OH	H	C	36
29	**40**	Br	H	OH	H	C	35
30	**41**	COOMe	H	OH	H	C	44
31	**42**	COOH	H	OH	H	C	(7) 30 [c]

[a] Yields calculated from the starting aldehyde **1**–**5** (see Scheme 1).
[b] Yield was improved up to 51% when THF was used as solvent instead of MeOH (9%).
[c] Yield was improved up to 30% when THF was used as solvent instead of MeOH (7%).

clearly translated into higher yields in the synthesis of 2,8-dioxabicyclo [3.3.1]nonane derivatives with a phloroglucinol moiety. In fact, some differences in yields were observed for dioxabicycles **29**–**34** (41–58 %) versus **39**–**42** (30–44 %), although they have not been observed for dioxabicycles with nitro group at A-ring, independently of the presence of a phloroglucinol moiety (**25**–**28**, entries 14–17 in Table 1) or a resorcinol one (**35**–**38**, entries 24–27 in Table 1). These results could be explained according to the highest electrophilic character of the corresponding flavylium salt that could be veiling the influence of the different nucleophilic properties of phloroglucinol (**21**) and resorcinol (**22**). In addition, no significant differences were observed in terms of yields between dioxabicycles with different substitution pattern at the C-ring, so yields for **25**, **26**, **35** and **36** (R_2 = H) (45–64 %) were similar to **27**, **28**, **37** and **38** ($R_2 = CH_3$) (50–64 %).

The structures of the synthesized compounds were characterized by IR, ^{1}H NMR, ^{13}C NMR, and 2D NMR spectroscopy as well as by HRMS spectrometry. Compounds **15**–**20**, **24**, **26** and **28**–**42** have been synthesized for the first time in this work and their structural characterization is now reported (^{1}H NMR and ^{13}C NMR spectra of the new compounds are included in the Supplementary Material section).

3.2. Inhibitory activity of 2,8-dioxabicyclo[3.3.1]nonanes 23–42 against hLDHA

The inhibitory effect of the 2,8-dioxabicyclo[3.3.1]nonane derivatives **23**–**42** over *h*LDHA catalytic activity, in the conversion of pyruvate to lactate, was evaluated by a UV spectrophotometric assay [34]. Briefly, the decrease in the co-substrate β-NADH absorbance at 340 nm (due to its oxidation into NAD^+) was measured for 10 min and the slope was compared with that obtained when no inhibitors were added (100 % enzymatic activity). The inhibitory activity of the commercial compound 3-[[3[(*cyclopropylamino*)*sulfonyl*]-7-(2,4-dimethoxy-5-pyrimidinyl)-4-quinolinyl]amino]-5-(3,5-difluorophenoxy)benzoic acid (GSK-2837808A) (Fig. 1) was also assessed to validate the method [28]. Moreover, the compound stiripentol (Fig. 1) was synthesized by us, according to the literature [55], and used as a reference, because of its known ability to decrease the urine oxalate excretion [18].

In a first screening assay, all synthesized compounds with the 2,8-dioxabicyclo[3.3.1]nonane scaffold and stiripentol were evaluated, at a single concentration of 50 μM, and the results were expressed as percentage of inhibition at that concentration (Table 2). Significant values, above 40 % of inhibition, were achieved for fifteen of them (**23**–**27**, **29**–**35**, **39**–**41**). However, compounds **28**, **36**–**38** and **42** showed low percentages of inhibition (31.5 %–38.1 %). The reference compound

Table 2
Percentage of inhibition against recombinant *h*LDHA of 2,8-dioxabicyclo[3.3.1]nonane derivatives (**23**–**42**) at a single concentration (50 μM), IC_{50} values against *h*LDHA of the most active compounds, IC_{50} values against *h*LDHB of a selection of compounds (**25**–**27**, **29**–**34**), and *in silico* prediction of partition coefficients (ClogP).

Compound	*h*LDHApercentage of inhibition (%) [a]	*h*LDHA IC_{50} (μM) [b]	R^2	*h*LDHB IC_{50} (μM) [b]	R^2	ClogP
23	41.7 ± 1.1	73.1 ± 2.5	0.87	ND[d]		2.74
24	43.0 ± 2.7	60.0 ± 4.7	0.92	ND[d]		3.23
25	68.4 ± 2.4	9.7 ± 1.1	0.93	28.6 ± 1.9	0.97	2.79
26	81.2 ± 2.4	24.4 ± 2.7	0.94	69.7 ± 4.7	0.95	3.27
27	72.0 ± 0.7	16.0 ± 1.7	0.97	18.1 ± 1.3	0.90	3.02
28	31.5 ± 7.7	> 100		ND[d]		3.50
29	64.2 ± 1.2	15.7 ± 2.7	0.94	39.7 ± 2.8	0.98	3.39
30	57.9 ± 3.5	26.7 ± 0.8	0.94	85.5 ± 2.5	0.98	3.88
31	84.5 ± 0.4	8.7 ± 0.8	0.95	23.8 ± 2.2	0.98	3.56
32	80.3 ± 0.5	15.4 ± 2.0	0.98	> 100		4.05
33	56.5 ± 3.9	26.7 ± 1.2	0.91	> 100		2.79
34	65.1 ± 1.7	20.0 ± 3.8	0.93	> 100		1.98
35	66.7 ± 2.6	35.8 ± 5.5	0.98	ND[d]		3.24
36	33.8 ± 2.8	> 100		ND[d]		3.73
37	38.1 ± 4.9	> 100		ND[d]		3.47
38	35.0 ± 2.7	> 100		ND[d]		3.96
39	84.1 ± 1.4	32.6 ± 1.3	0.97	ND[d]		3.84
40	88.5 ± 2.5	33.4 ± 5.5	0.95	ND[d]		4.02
41	41.3 ± 1.5	83.7 ± 14.4	0.94	ND[d]		3.24
42	38.1 ± 4.9	> 100		ND[d]		2.44
Stiripentol [c]	5.9 ± 0.9	> 100		ND[d]		

[a] Data are presented as the mean ± SD of $n = 4$ replicates for percentage of inhibition.
[b] Data are presented as the mean ± SD of $n = 3$ replicates for IC_{50} values.
[c] The compound (*E*)-1-(benzo[*d*][1,3]dioxol-5-yl)-4,4-dimethylpent-1-en-3-ol (stiripentol) was used as a reference.
[d] Not determined (ND) as the IC_{50} values against *h*LDHA was above 30 μM.

stiripentol showed a value below 10 %. For a second assay, eight different concentrations, in a range between 0 and 200 μM, were prepared from compounds **23**–**27**, **29**–**35**, and **39**–**41**, and a dose response curve fitting the logarithm of inhibitor concentration *vs* normalized enzymatic activity have allowed to determine IC_{50} values for each of them (Table 2).

2,8-Dioxabicyclo[3.3.1]nonane derivatives with a phloroglucinol moiety and a nitro, chloro, bromo, carboxylic or carboxymethyl group at the A-ring (**25**–**27**, **29**–**34**) were the most active compounds. They showed IC_{50} values in the range of 8.7–26.7 μM, standing up among them **25** (IC_{50} = 9.7 μM) and **31** (IC_{50} = 8.7 μM) (Table 2). However, the IC_{50} value of compound **28**, whose structure is close to the previous ones, was exceptionally high (>100 μM). On the other hand, the values obtained for compounds with a resorcinol moiety (**35**–**42**) were higher, in the range of 32.6–83.7 μM for **35** and **39**–**41**, and much higher (>100 μM) for **36**–**38** and **42**. This effect of phloroglucinol or resorcinol moieties on the inhibitory activity of the corresponding dioxabicycles was notably observed on compounds with carboxylic and carboxymethyl groups at A-ring (**33**, **34**, **41**, and **42**). Thus, the IC_{50} values of **33** and **34** (26.7 and 20.0 μM, respectively) versus **41** and **42** (83.7 and above 100 μM, respectively) confirmed it. Finally, compounds without substitution at A-ring (**23** and **24**) showed low activity, with IC_{50} values above 50 μM (Table 2). In summary, compounds **23**–**27**, **29**–**35**, and **39**–**41** are better LDHAi's than related polyphenolics, such as galloflavin (IC_{50} = 103.6 μM) or luteolin-7-*O*-β-D-glucopiranoside (IC_{50} = 139.2 μM) [33].

In addition, theoretical partition coefficients, expressed as ClogP, corresponding to un-ionized species, were calculated to estimate the lipophilicity of the synthesized compounds and the cell membrane permeability [56]. Favorable values, between 0 and 5, were obtained for all the dioxabicycles **23**–**42** (Table 2).

3.3. Inhibitory activity of 2,8-dioxabicyclo[3.3.1]nonane derivatives 25–27 and 29–34 against hLDHB

The *h*LDHB inhibitory activities of our most active *h*LDHA inhibitors (**25**–**27** and **29**–**34**) were also measured and, according to the IC_{50} values obtained for these compounds (Table 2), all of them showed higher concentrations for the 50 % inhibition of *h*LDHB than for the 50 % inhibition of *h*LDHA, which means they have certain selectivity inhibiting *h*LDHA versus *h*LDHB. In particular, the most active *h*LDHA inhibitors (**25**, **29**, **31**) showed a selectivity (*h*LDHB/*h*LDHA IC_{50}) of 3.0, 2.5, and 2.7, respectively. This general positive result is more favorable for compounds **32** and **34**, since their IC_{50} values against *h*LDHB are 6.5 and 5.0 times higher than the corresponding *h*LDHA IC_{50} values, respectively.

3.4. In vitro effectiveness of LDHAi's (25, 29, 31) in reducing oxalate output in hyperoxaluric mouse hepatocytes (Agxt1$^{-/-}$, Grhpr$^{-/-}$, Hoga1$^{-/-}$)

The generation of *Agxt1*$^{-/-}$, *Grhpr*$^{-/-}$, *Hoga1*$^{-/-}$ mice by either gene targeting or gene trapping has been described previously [53,57,58]. Hyperoxaluric mice excrete high levels of oxalate in the urine. To enhance hepatocytes oxalate output, glycolate has been added to the *Agxt1*$^{-/-}$ and *Grhpr*$^{-/-}$ primary hepatocyte cultures and hydroxyproline to the *Hoga1*$^{-/-}$ primary hepatocyte culture.

In this work, the capacity of three of the most active LDHAi's (**25**, **29**, **31**) to reduce oxalate production in *Agxt1*$^{-/-}$, *Grhpr*$^{-/-}$ or *Hoga1*$^{-/-}$ mouse primary hepatocytes cell culture has been evaluated according to previously reported methodology [7,53]. Stiripentol has been selected as reference in the assay. Values of relative oxalate output of *Agxt1*$^{-/-}$, *Grhpr*$^{-/-}$ or *Hoga1*$^{-/-}$ mouse primary hepatocyte cells, in the presence of **25**, **29**, **31** or stiripentol at a concentration of 10 μM, are shown in Table 3. After 24 h of treatment with stiripentol, the oxalate level in *Agxt1*$^{-/-}$ and *Grhpr*$^{-/-}$ cells was reduced up to 24 % and 27 %, respectively. Compounds **25** and **29** showed a similar behavior to that of stiripentol, while compound **31** showed lower activity than that reference compound in *Agxt1*$^{-/-}$ and *Grhpr*$^{-/-}$ cells (35 % and 65 % of relative oxalate output, respectively).

Regarding *Hoga1*$^{-/-}$ cells, an efficient decrease in oxalate level was observed at 24-h treatment with compounds **25** and **31** (16 % and 19 % of relative oxalate output, respectively), respect to that observed with stiripentol (70 %). However, these favorable results were lost at 48 h. In any case, although compound **25** lose activity, the relative oxalate output at 48 h of treatment with such compound is similar to that with stiripentol at the same time. Therefore, the advantage over stiripentol is

Table 3
Biological data[a] of the 2,8-dioxabicyclo[3.3.1]nonane derivatives **25**, **29** and **31**: relative excreted oxalate[b] in *Agxt1*$^{-/-}$, *Grhpr*$^{-/-}$ or *Hoga1*$^{-/-}$ mouse primary hepatocytes cell culture.

	Compound			
	25 (10 μM)	**29** (10 μM)	**31** (10 μM)	Stiripentol (10 μM)
PH1 model (*Agxt1*$^{-/-}$ mouse primary hepatocytes cell culture)				
Relative oxalate (24 h)	27 ± 18	25 ± 16	35 ± 7	24 ± 7
Relative oxalate (48 h)	59 ± 1	59 ± 4	71 ± 5	63 ± 8
PH2 model (*Grhpr*$^{-/-}$ mouse primary hepatocytes cell culture)				
Relative oxalate (24 h)	29 ± 8	29 ± 6	65 ± 8	27 ± 8
Relative oxalate (48 h)	70 ± 26	55 ± 14	78 ± 4	33 ± 1
PH3 model (*Hoga1*$^{-/-}$ mouse primary hepatocytes cell culture)				
Relative oxalate (24 h)	16 ± 14	37 ± 7	19 ± 14	70 ± 4
Relative oxalate (48 h)	52 ± 37	57 ± 7	69 ± 26	49 ± 5

[a] Data are represented as the mean ± SD of $n = 3$ replicates.
[b] Relative excreted oxalate is the oxalate concentration found in the extracellular medium after treatment with an inhibitor with respect to the oxalate concentration found in the extracellular medium in the absence of the inhibitor, expressed as a percentage.

obvious, since **25** is more potent than stiripentol at least at 24 h. The reasons for this decay in activity are likely complex and unknown at the moment. It could be due to the loss of concentration of these compounds as a result of their metabolization and/or degradation. We also need to keep in mind that the primary culture of mouse hepatocytes is a short-term system, since it is our experience that these hepatocytes change their gene expression profile after about a week of culture.

Cells did not show any sign of cytotoxicity at the concentration tested (10 μM) of **25**, **29**, **31** and stiripentol, since no significant differences in the mean values with respect to control wells were observed.

4. Conclusion

The present study reports on the synthesis of twenty compounds (**23**–**42**) with a 2,8-dioxabicyclo[3.3.1]nonane scaffold, which is present in bioactive natural A-type proanthocyanidins, on their selective *h*LDHA inhibitory activity, and on the effectiveness of some of them in reducing oxalate output in hyperoxaluric mouse (*Agxt1*$^{-/-}$, *Grhpr*$^{-/-}$, *Hoga1*$^{-/-}$) hepatocytes. A two-step synthetic method through flavylium salts has been performed according to procedures previously used by us. The overall reaction yields for **23**–**42** have been calculated from starting materials (aldehydes) and better values (30–64 %) are achieved when electron-withdrawing groups (NO_2, Cl, Br, COOH and COOMe) were present at the A-ring. To our knowledge, this is the first time that A-type proanthocyanidin analogues have been evaluated as *h*LDHA inhibitors. We have observed that several compounds with a catechol/hydroxyphenyl moiety (B-ring) and a phloroglucinol unit linked to C-ring (**25**–**27**, **29**–**34**) present experimental IC_{50} values lower than 30 μM against *h*LDHA. Among all of them, compounds **25** ($IC_{50} = 9.7$ μM) and **31** ($IC_{50} = 8.7$ μM) can be highlighted, since they are 10-fold more potent *h*LDHA inhibitors than other polyphenolic flavone-based inhibitors, such as galloflavin and luteolin-7-*O*-β-D-glucopiranoside. In order to know the selectivity of compounds **25**–**27**, **29**–**34** towards *h*LDHA, their *h*LDHB inhibitory activities were also measured, showing all of them higher *h*LDHB IC_{50} values. In particular, compounds **32** and **34** showed IC_{50} values against *h*LDHB around 6.5 and 5.0 times higher than the corresponding *h*LDHA IC_{50} values, respectively. In addition, a greater activity of compounds **25** and **31** compared to stiripentol was observed at 24 h in the PH3 model (*Hoga1*$^{-/-}$ hepatocytes cell culture). Cells did not show any sign of cytotoxicity at the concentration tested (10 mM). All these results lead to select **25**, **29**, and **31** as hits for structural optimization in future preparations of more potent *h*LDHA inhibitors for the potential treatment of primary hyperoxalurias. Isoform selectivity (LDHA *vs* LDHB) will be also considered as a relevant goal in drug development. In addition, an important limitation of systemic LDH inhibition is the potential unwanted effects on tissues other than the liver. The mild phenotype of genetically deficient LDHA or LDHB patients (https://medlineplus.gov/genetics/condition/lactate-dehydrogenase-deficiency) is supportive of cautious optimism. Nonetheless, it will be necessary to continue exploring the developing nanocarrier-based drug delivery systems to efficiently deliver these compounds into the hepatic cells.

Declaration of Competing Interest

The authors declare that they have no known competing financial interests or personal relationships that could have appeared to influence the work reported in this paper.

Acknowledgements

The authors wish to thank the Spanish *Ministerio de Ciencia, Innovación y Universidades* (grants RTI2018-098560-B-C21 and RTI2018-098560-B-C22, co-financed by the FEDER funds of the European Union) for financial support and the *Centro de Instrumentación Científico-Técnica* (CICT) of the University of Jaén, Spain, for partial financial support. A. A.-A. was the recipient of a predoctoral fellowship granted by the University of Jaén and is currently contracted by the Andalusian *Consejería de Economía y Conocimiento* (FEDER program 2014-2020: grant number 1380682). C. C. was the recipient of a European Youth Guarantee contract. Authors also wish to thank Dr. Cristina Martín-Higueras and Dr. Mª Dolores Moya-Garzón by their advices with the *h*LDHA assay.

Appendix A. Supplementary data

Supplementary data to this article can be found online at https://doi.org/10.1016/j.bioorg.2022.106127.

References

[1] E. Salido, A.L. Pey, R. Rodriguez, V. Lorenzo, Primary hyperoxalurias: Disorders of glyoxylate detoxification, Biochim. Biophys. Acta-Mol. Basis Dis. 1822 (9) (2012) 1453–1464, https://doi.org/10.1016/j.bbadis.2012.03.004.
[2] J.R. Ingelfinger, P. Cochat, G. Rumsby, Primary hyperoxaluria, N. Engl. J. Med. 369 (7) (2013) 649–658, https://doi.org/10.1056/NEJMra1301564.
[3] P. Cochat, S.-A. Hulton, C. Acquaviva, C.J. Danpure, M. Daudon, M. De Marchi, S. Fargue, J. Groothoff, J. Harambat, B. Hoppe, N.V. Jamieson, M.J. Kemper, G. Mandrile, M. Marangella, S. Picca, G. Rumsby, E. Salido, M. Straub, C.S. van Woerden, Primary hyperoxaluria Type 1: Indications for screening and guidance for diagnosis and treatment, Nephrol. Dial. Transplant. 27 (5) (2012) 1729–1736, https://doi.org/10.1093/ndt/gfs078.
[4] C. Martin-Higueras, A. Torres, E. Salido, Molecular therapy of primary hyperoxaluria, J. Inherit. Metab. Dis. 40 (4) (2017) 481–489, https://doi.org/10.1007/s10545-017-0045-3.
[5] M.D. Moya-Garzón, J.A. Gómez-Vidal, A. Alejo-Armijo, J. Altarejos, J. R. Rodríguez-Madoz, M.X. Fernandes, E. Salido, S. Salido, M. Díaz-Gavilán, Small molecule-based enzyme inhibitors in the treatment of primary hyperoxalurias, J. Pers. Med. 11 (2021) 74, https://doi.org/10.3390/jpm11020074.
[6] K. Shee, M.L. Stoller, Perspectives in primary hyperoxaluria — historical, current and future clinical interventions, Nat. Rev. Urol. 19 (3) (2022) 137–146, https://doi.org/10.1038/s41585-021-00543-4.
[7] C. Martin-Higueras, S. Luis-Lima, E. Salido, Glycolate oxidase is a safe and efficient target for substrate reduction therapy in a mouse model of primary hyperoxaluria type I, Mol. Ther. 24 (4) (2016) 719–725, https://doi.org/10.1038/mt.2015.224.
[8] C. Dutta, N. Avitahl-Curtis, N. Pursell, M. Larsson Cohen, B. Holmes, R. Diwanji, W. Zhou, L. Apponi, M. Koser, B.o. Ying, D. Chen, X. Shui, U. Saxena, W.A. Cyr, A. Shah, N. Nazef, W. Wang, M. Abrams, H. Dudek, E. Salido, B.D. Brown, C. Lai, Inhibition of glycolate oxidase with dicer-substrate siRNA reduces calcium oxalate deposition in a mouse model of primary hyperoxaluria type 1, Mol. Ther. 24 (4) (2016) 770–778, https://doi.org/10.1038/mt.2016.4.
[9] M.D. Moya-Garzón, C. Martín Higueras, P. Peñalver, M. Romera, M.X. Fernandes, F. Franco-Montalbán, J.A. Gómez-Vidal, E. Salido, M. Díaz-Gavilán, Salicylic acid derivatives inhibit oxalate production in mouse hepatocytes with primary hyperoxaluria type 1, J. Med. Chem. 61 (16) (2018) 7144–7167, https://doi.org/10.1021/acs.jmedchem.8b00399.
[10] C.B. Summitt, L.C. Johnson, T.J. Jönsson, D. Parsonage, R.P. Holmes, W. T. Lowther, Proline dehydrogenase 2 (PRODH2) is a hydroxyproline

dehydrogenase (HYPDH) and molecular target for treating primary hyperoxaluria, Biochem. J. 466 (2015) 273–281, https://doi.org/10.1042/BJ20141159.
[11] W.T. Lowther, R. Holmes, Combinations for the treatment of kidney stones, U.S. Patent WO2017100268, 15 June 2017.
[12] C. Lai, N. Pursell, J. Gierut, U. Saxena, W. Zhou, M. Dills, R. Diwanji, C. Dutta, M. Koser, N. Nazef, R. Storr, B. Kim, C. Martin-Higueras, E. Salido, W. Wang, M. Abrams, H. Dudek, B.D. Brown, Specific inhibition of hepatic lactate dehydrogenase reduces oxalate production in mouse models of primary hyperoxaluria, Mol. Ther. 26 (8) (2018) 1983–1995, https://doi.org/10.1016/j.ymthe.2018.05.016.
[13] B. Hoppe, A. Koch, P. Cochat, S.F. Garrelfs, M.A. Baum, J.W. Groothoff, G. Lipkin, M. Coenen, G. Schalk, A. Amrite, D. McDougall, K. Barrios, C.B. Langman, Safety, pharmacodynamics, and exposure-response modeling results from a first-in-human phase 1 study of nedosiran (PHYOX1) in primary hyperoxaluria, Kidney Int. 101 (3) (2022) 626–634, https://doi.org/10.1016/j.kint.2021.08.015.
[14] T.A. Forbes, B.D. Brown, C. Lai, Therapeutic RNA interference: A novel approach to the treatment of primary hyperoxaluria, Br. J. Clin. Pharmacol. 88 (6) (2022) 2525–2538, https://doi.org/10.1111/bcp.14925.
[15] G. Ariceta, K. Barrios, B.D. Brown, B. Hoppe, R. Rosskamp, C.B. Langman, Hepatic Lactate Dehydrogenase A: An RNA Interference Target for the Treatment of All Known Types of Primary Hyperoxaluria, Kidney Int. Rep. 6 (4) (2021) 1088–1098, https://doi.org/10.1016/j.ekir.2021.01.029.
[16] M.S. Murray, R.P. Holmes, W.T. Lowther, Active site and loop 4 movements within human glycolate oxidase: Implications for substrate specificity and drug design, Biochemistry 47 (2008) 2439–2449, https://doi.org/10.1021/bi701710r.
[17] E.C.Y. Lee, A.J. McRiner, K.E. Georgiadis, J. Liu, Z. Wang, A.D. Ferguson, B. Levin, M. von Rechenberg, C.D. Hupp, M.I. Monteiro, A.D. Keefe, A. Olszewski, C. J. Eyermann, P. Centrella, Y. Liu, S. Arora, J.W. Cuozzo, Y. Zhang, M.A. Clark, C. Huguet, A. Kohlmann, Discovery of novel, potent inhibitors of hydroxy acid oxidase 1 (HAO1) using DNA-encoded chemical library screening, J. Med. Chem. 64 (10) (2021) 6730–6744, https://doi.org/10.1021/acs.jmedchem.0c02271.
[18] M. Le Dudal, L. Huguet, J. Pérez, S. Vandermeersch, E. Bouderlique, E. Tang, C. Martori, N. Chemaly, R. Nabbout, J.-P. Haymann, V. Frochot, L. Baud, G. Deschênes, M. Daudon, E. Letavernier, Stiripentol protects against calcium oxalate nephrolithiasis and ethylene glycol poisoning, J. Clin. Invest. 129 (2019) 2571–2577, https://doi.org/10.1172/JCI99822.
[19] C. Kempf, A. Pfau, J. Holle, K. Müller-Schlüter, P. Bufler, F. Knauf, D. Müller, Stiripentol fails to lower plasma oxalate in a dialysis-dependent PH1 patient, Pediatr. Nephrol. 35 (9) (2020) 1787–1789, https://doi.org/10.1007/s00467-020-04585-5.
[20] C.M. Wyatt, T.B. Drüeke, Stiripentol for the treatment of primary hyperoxaluria and calcium oxalate nephropathy, Kidney Int. 97 (1) (2020) 17–19, https://doi.org/10.1016/j.kint.2019.06.011.
[21] Clinical trials available online: https://clinicaltrials.gov/ (accessed 10 April 2022).
[22] M.D. Moya-Garzon, B. Rodriguez-Rodriguez, C. Martin-Higueras, F. Franco-Montalban, M.X. Fernandes, J.A. Gomez-Vidal, A.L. Pey, E. Salido, M. Diaz-Gavilan, New salicylic acid derivatives, double inhibitors of glycolate oxidase and lactate dehydrogenase, as effective agents decreasing oxalate production, Eur. J. Med. Chem. 237 (2022) 114396, https://doi.org/10.1016/j.ejmech.2022.114396.
[23] J. Ding, R. Gumpena, M.-O. Boily, A. Caron, O. Chong, J.H. Cox, V. Dumais, S. Gaudreault, A.H. Graff, A. King, J. Knight, R. Oballa, J. Surendradoss, T. Tang, J. Wu, W.T. Lowther, D.A. Powell, Dual glycolate oxidase/lactate dehydrogenase A inhibitors for primary hyperoxaluria, ACS Med. Chem. Lett. 12 (7) (2021) 1116–1123, https://doi.org/10.1021/acsmedchemlett.1c0019610.1021/acsmedchemlett.1c00196.s001.
[24] M.V. Liberti, J.W. Locasale, The warburg effect: How does it benefit cancer cells? Trends Biochem. Sci. 41 (3) (2016) 211–218, https://doi.org/10.1016/j.tibs.2015.12.001.
[25] R. Rani, V. Kumar, Recent update on human lactate dehydrogenase enzyme 5 (hLDH5) inhibitors: A promising approach for cancer chemotherapy, J. Med. Chem. 59 (2) (2016) 487–496, https://doi.org/10.1021/acs.jmedchem.5b00168.
[26] M.R. Woodford, V.Z. Chen, S.J. Backe, G. Bratslavsky, M. Mollapour, Structural and functional regulation of lactate dehydrogenase-A in cancer, Future Med. Chem. 12 (5) (2020) 439–455, https://doi.org/10.4155/fmc-2019-0287.
[27] G. Rai, D.J. Urban, B.T. Mott, X. Hu, S.-M. Yang, G.A. Benavides, M.S. Johnson, G. L. Squadrito, K.R. Brimacombe, T.D. Lee, D.M. Cheff, H.u. Zhu, M.J. Henderson, K. Pohida, G.A. Sulikowski, D.M. Dranow, M.d. Kabir, P. Shah, E. Padilha, D. Tao, Y. Fang, P.P. Christov, K. Kim, S. Jana, P. Muttil, T. Anderson, N.K. Kunda, H. J. Hathaway, D.F. Kusewitt, N. Oshima, M. Cherukuri, D.R. Davies, J.P. Norenberg, L.A. Sklar, W.J. Moore, C.V. Dang, G.M. Stott, L. Neckers, A.J. Flint, V.M. Darley-Usmar, A. Simeonov, A.G. Waterson, A. Jadhav, M.D. Hall, D.J. Maloney, Pyrazole-based lactate dehydrogenase inhibitors with optimized cell activity and pharmacokinetic properties, J. Med. Chem. 63 (19) (2020) 10984–11011, https://doi.org/10.1021/acs.jmedchem.0c00916.
[28] J. Billiard, J.B. Dennison, J. Briand, R.S. Annan, D. Chai, M. Colón, C.S. Dodson, S. A. Gilbert, J. Greshock, J. Jing, H. Lu, J.E. McSurdy-Freed, L.A. Orband-Miller, G. B. Mills, C.J. Quinn, J.L. Schneck, G.F. Scott, A.N. Shaw, G.M. Waitt, R.F. Wooster, K.J. Duffy, Quinoline 3-sulfonamides inhibit lactate dehydrogenase A and reverse aerobic glycolysis in cancer cells, Cancer Metab. 1 (2013) 2–17, https://doi.org/10.1186/2049-3002-1-19.
[29] H.E. Purkey, K. Robarge, J. Chen, Z. Chen, L.B. Corson, C.Z. Ding, A.G. DiPasquale, P.S. Dragovich, C. Eigenbrot, M. Evangelista, B.P. Fauber, Z. Gao, H. Ge, A. Hitz, Q. Ho, S.S. Labadie, K.W. Lai, W. Liu, Y. Liu, C. Li, S. Ma, S. Malek, T. O'Brien, J. Pang, D. Peterson, L. Salphati, S. Sideris, M. Ultsch, BinQing Wei, I. Yen, Q. Yue, H. Zhang, A. Zhou, Cell active hydroxylactam inhibitors of human lactate dehydrogenase with oral bioavailability in mice, ACS Med. Chem. Lett. 7 (10) (2016) 896–901, https://doi.org/10.1021/acsmedchemlett.6b00190.
[30] E. Mazzio, K. Soliman, Inhibition of anaerobic glucose metabolism and corresponding natural composition as a non-toxic approach to cancer treatment, U. S. Patent WO2006017494, 2 August 2004.
[31] Z. Wang, D. Wang, S. Han, N. Wang, F. Mo, T.Y. Loo, J. Shen, H. Huang, J. Chen, L.-Z. Sun, Bioactivity-guided identification and cell signaling technology to delineate the lactate dehydrogenase A inhibition effects of *Spatholobus suberectus* on breast cancer, PLoS One 8 (2) (2013) e56631, https://doi.org/10.1371/journal.pone.0056631.
[32] M. Manerba, M. Vettraino, L. Fiume, G. DiStefano, A. Sartini, E. Giacomini, R. Buonfiglio, M. Roberti, M. Recanatini, Galloflavin (CAS 568–80-9): A novel inhibitor of lactate dehydrogenase, ChemMedChem 7 (2) (2012) 311–317, https://doi.org/10.1002/cmdc.201100471.
[33] A. Bader, T. Tuccinardi, C. Granchi, A. Martinelli, M. Macchia, F. Minutolo, N. De Tommasi, A. Braca, Phenylpropanoids and flavonoids from *Phlomis kurdica* as inhibitors of human lactate dehydrogenase, Phytochemistry 116 (2015) 262–268, https://doi.org/10.1016/j.phytochem.2015.03.007.
[34] W. Li, J. Liu, R. Guan, J. Chen, D. Yang, Z. Zhao, D. Wang, Chemical characterization of procyanidins from *Spatholobus suberectus* and their antioxidative and anticancer activities, J. Funct. Food. 12 (2015) 468–477, https://doi.org/10.1016/j.jff.2014.11.009.
[35] A. Alejo-Armijo, N. Glibota, M.P. Frías, J. Altarejos, A. Gálvez, E. Ortega-Morente, S. Salido, Antimicrobial and antibiofilm activities of procyanidins extracted from laurel wood against a selection of foodborne microorganisms, Int. J. Food Sci. Technol. 52 (3) (2017) 679–686, https://doi.org/10.1111/ijfs.13321.
[36] A. Alejo-Armijo, A. Tello-Abolafia, S. Salido, J. Altarejos, Phenolic compounds in laurel wood: A new source of proanthocyanidins, J. Wood Chem. Technol. 39 (6) (2019) 436–453, https://doi.org/10.1080/02773813.2019.1636825.
[37] J. Ortega-Vidal, A. Cobo, E. Ortega-Morente, A. Gálvez, M. Martínez-Bailén, S. Salido, J. Altarejos, Antimicrobial activity of phenolics isolated from the pruning wood residue of European plum (*Prunus domestica* L.), Ind. Crop. Prod. 176 (2022) 114296, https://doi.org/10.1016/j.indcrop.2021.114296.
[38] A. Alejo-Armijo, A.J. Parola, F. Pina, J. Altarejos, S. Salido, Thermodynamic stability of flavylium salts as a valuable tool to design the synthesis of A-type proanthocyanidin analogues, J. Org. Chem. 83 (19) (2018) 12297–12304, https://doi.org/10.1021/acs.joc.8b0178010.1021/acs.joc.8b01780.s001.
[39] A. Alejo-Armijo, N. Glibota, M.P. Frías, J. Altarejos, A. Gálvez, S. Salido, E. Ortega-Morente, Synthesis and evaluation of antimicrobial and antibiofilm properties of A-type procyanidin analogues against resistant bacteria in food, J. Agric. Food Chem. 66 (9) (2018) 2151–2158, https://doi.org/10.1021/acs.jafc.8b0053510.1021/acs.jafc.8b00535.s001.
[40] A. Rauf, M. Imran, T. Abu-Izneid, S. Iahtisham-Ul-Haq, X. Patel, S. Pan, A.S. Naz, F. Silva, H.A.R. Saeed, P. Suleria, A comprehensive review, Biomed. Pharmacother. 116 (2019), 108999, https://doi.org/10.1016/j.biopha.2019.108999.
[41] A. Alejo-Armijo, S. Salido, Joaquín Altarejos, Synthesis of A-type proanthocyanidins and their analogues: A comprehensive review, J. Agric. Food Chem. 68 (31) (2020) 8104–8118, https://doi.org/10.1021/acs.jafc.0c03380.
[42] G. Yin, T. Ren, Y. Rao, Y. Zhou, Z. Li, W. Shu, A. Wu, Stereoselective synthesis of 2,8-dioxabicyclo[3.3.1]nonane derivatives via a sequential Michael addition/bicyclization reaction, J. Org. Chem. 78 (7) (2013) 3132–3141, https://doi.org/10.1021/jo400081q.
[43] N.C. Ganguly, P. Mondal, S. Roy, A mild efficient iodine-catalyzed synthesis of novel anticoagulants with 2,8-dioxabicyclo[3.3.1]nonane core, Tetrahedron Lett. 54 (19) (2013) 2386–2390, https://doi.org/10.1016/j.tetlet.2013.02.092.
[44] X. Jiang, Z. Song, C. Xu, Q. Yao, A. Zhang, (D,L)-10-Camphorsulfonic-acid-catalysed synthesis of diaryl-fused 2,8-dioxabicyclo[3.3.1]nonanes from 2-hydroxychalcones and naphthol derivatives, Eur. J. Org. Chem. 2014 (2014) 418–425. https://doi.org/10.1002/ejoc.201301295.
[45] L. Xia, H. Cai, Y.R. Lee, Catalyst-controlled regio- and stereoselective synthesis of diverse 12H–6,12-methanodibenzo[d, g][1,3]dioxocines, Org. Biomol. Chem. 12 (25) (2014) 4386–4396, https://doi.org/10.1039/C4OB00691G.
[46] A. Alejo-Armijo, S. Salido, J. Altarejos, A.J. Parola, S. Gago, N. Basílio, L. Cabrita, F. Pina, Effect of methyl, hydroxyl, and chloro substituents in position 3 of 3′,4′,7-trihydroxyflavylium: Stability, kinetics, and thermodynamics, Chem. Eur. J. 22 (35) (2016) 12495–12505, https://doi.org/10.1002/chem.201601564.
[47] W.L.F. Armarego, Purification of Laboratory Chemicals, eighth ed., Butterworth-Heinemann, Burlington, 2017.
[48] G. Calogero, A. Sinopoli, I. Citro, G. Di Marco, V. Petrov, A.M. Diniz, A.J. Parola, F. Pina, Synthetic analogues of anthocyanins as sensitizers for dye-sensitized solar cells, Photochem. Photobiol. Sci. 12 (5) (2013) 883.
[49] F. Pina, A. Roque, M.J. Melo, M. Maestri, L. Belladelli, V. Balzani, Multistate/multifunctional molecular-level systems: Light and pH switching between the various forms of a synthetic flavylium salt, Chem. Eur. J. 4 (1998) 1184–1191, https://doi.org/10.1002/(SICI)1521-3765(19980710)4:7<1184::AID-CHEM1184>3.0.CO;2-6.
[50] M.C. Moncada, A.J. Parola, C. Lodeiro, F. Pina, M. Maestri, V. Balzani, Multistate/multifunctional behaviour of 4′-hydroxy-6-nitroflavylium: A write-lock/read/unlock/enable-erase/erase cycle driven by light and pH stimulation, Chem. Eur. J. 10 (6) (2004) 1519–1526, https://doi.org/10.1002/chem.200305348.
[51] M. Kraus, E. Biskup, E. Richling, P. Schreier, Synthesis of [4-14C]-pelargonidin chloride and [4-^{14}C]-delphinidin chloride, J. Label. Compd. Radiopharm. 49 (13) (2006) 1151–1162, https://doi.org/10.1002/jlcr.1120.
[52] MOE (molecular operating environment) 2020 software (Chemical Computing Group, ULC, Canada).

[53] E.C. Salido, X.M. Li, Y. Lu, X. Wang, A. Santana, N. Roy-Chowdhury, A. Torres, L. J. Shapiro, J. Roy-Chowdhury, Alanine-glyoxylate aminotransferase-deficient mice, a model for primary hyperoxaluria that responds to adenoviral gene transfer, Proc. Natl. Acad. Sci. 103 (48) (2006) 18249–18254, https://doi.org/10.1073/pnas.0607218103.

[54] G. Kraus, Y. Yuan, A. Kempema, A Convenient synthesis of type A procyanidins, Molecules 14 (2009) 807–815, https://doi.org/10.3390/molecules14020807.

[55] M.S. Almutairi, D.R. Leenaraj, H.A. Ghabbour, I.H. Joe, M.I. Attia, Spectroscopic identification, structural features, Hirshfeld surface analysis and molecular docking studies on stiripentol: An orphan antiepileptic drug, J. Mol. Struct. 1180 (2019) 110–118, https://doi.org/10.1016/j.molstruc.2018.11.088.

[56] C.A. Lipinski, F. Lombardo, B.W. Dominy, P.J. Feeney, Experimental and computational approaches to estimate solubility and permeability in drug discovery and development settings, Adv. Drug Deliv. Rev. 23 (1-3) (1997) 3–25, https://doi.org/10.1016/S0169-409X(96)00423-1.

[57] J. Knight, R.P. Holmes, S.D. Cramer, T. Takayama, E. Salido, Hydroxyproline metabolism in mouse models of primary hyperoxaluria, Am. J. Physiol.-Renal Physiol. 302 (6) (2012) F688–F693, https://doi.org/10.1152/ajprenal.00473.2011.

[58] X. Li, J. Knight, W. Todd Lowther, R.P. Holmes, Hydroxyproline metabolism in a mouse model of primary hyperoxaluria type 3, Biochim. Biophys. Acta-Mol. Basis Dis. 1852 (12) (2015) 2700–2705, https://doi.org/10.1016/j.bbadis.2015.09.016.